

Retinol dehydrogenase-10 regulates pancreas organogenesis and endocrine cell differentiation via paracrine retinoic acid signalling

Igor Arregi^{1¶}, Maria Climent^{1¶}, Dobromir Iliev¹, Jürgen Strasser¹, Nadège Gouignard¹, Jenny K. Johansson¹, Tania Singh¹, Magdalena Mazur¹, Henrik Semb², Isabella Artner¹, Lilitiana Minichiello³, Edgar M. Pera^{1*}

¹ Lund Stem Cell Center, Lund University, Lund, Sweden

² The Danish Stem Cell Center, University of Copenhagen, Copenhagen, Denmark

³ Department of Pharmacology, University of Oxford, Oxford, United Kingdom

[¶] These authors contributed equally to this work.

Abbreviated Title: Rdh10 in pancreatic endocrine cell differentiation

Keywords: Retinoic acid, pancreas development, endocrine cell, mouse

Word Count: (excl. abstract, figure captions, and references) 5921

Number of figures and tables: 9

Corresponding author and person to whom reprint requests should be addressed:

Edgar M. Pera, Ph.D.

Lund Stem Cell Center

Lund University

BMC, D10, Klinikgatan 32, SE-22184 Lund, Sweden

Phone: +46-46-2221738

Fax: +46-46-2220296

e-mail: edgar.pera@med.lu.se

Grants and fellowships: E.M.P was funded by grants of the Swedish Research Council, Novo Nordisk Foundation, Swedish Diabetes Foundation, and Director Albert Pålsson Foundation; I. Arregi was funded by a Wenner Gren foundation fellowship and Craaford foundation grant.

Disclosure Statement: The authors have nothing to disclose.

Abstract

Vitamin A-derived retinoic acid (RA) signals are critical for the development of several organs, including the pancreas. However, the tissue-specific control of RA synthesis in organ development and cell differentiation has only poorly been addressed *in vivo*. Here we show that Retinol dehydrogenase-10 (Rdh10), a key enzyme in embryonic RA production, has important functions in pancreas organogenesis and endocrine cell differentiation. *Rdh10* is expressed in the developing pancreas epithelium and surrounding mesenchyme. *Rdh10* null mutant mouse embryos exhibited dorsal pancreas agenesis and a hypoplastic ventral pancreas with retarded tubulogenesis and branching. Conditional disruption of *Rdh10* from the endoderm caused increased mortality, reduced body weight and lowered blood glucose levels after birth. Endodermal *Rdh10* deficiency led to a smaller dorsal pancreas with a reduced density of early glucagon⁺ and insulin⁺ cells. During the secondary transition, the reduction of Neurogenin3⁺ endocrine progenitors in the mutant dorsal pancreas accounted for fewer α - and β -cells. Changes in the expression of α - and β -cell-specific transcription factors indicated that *Rdh10* might also participate in the terminal differentiation of endocrine cells. Together, our results highlight the importance of both mesenchymal and epithelial *Rdh10* for pancreogenesis and early endocrine cell differentiation. We further propose a model in which the *Rdh10*-expressing exocrine tissue is introduced as an essential source of RA signals in late endocrine cell differentiation.

Introduction

Tissue interactions play a major role in organ development and cellular differentiation. The endodermally-derived pancreas develops in close association with tissues of mesodermal origin. Later, the islets of Langerhans, constituting the endocrine compartment with important glucose-regulating functions, form adjacent to exocrine cells in the pancreatic epithelium. While transcription factors in the developing pancreas and endocrine cells have been extensively studied, less is known about how extrinsic signals regulate their expression (1-3). A deeper understanding of paracrine

signalling in pancreas development and endocrine cell differentiation in the developing embryo is needed for successful cell-replacement therapies in diabetes.

In the mouse, the pancreas becomes morphologically apparent at embryonic days 9.0 and 9.5 (E9.0-E9.5) as dorsal and ventral evaginations of the posterior foregut endoderm (4). The dorsal pancreas is induced by signals from the overlying notochord, dorsal aorta and dorsal mesenchyme. On the ventral side of the foregut, the ventral pancreas segregates from the adjacent liver primordium under the influence of signals from the cardiac and septum transversum mesoderm. The early pancreatic buds that eventually fuse to become a single organ encompass multipotent progenitor cells (MPCs) that give rise to both exocrine (acinar/ductal) and endocrine tissue (5,6). Ablation of MPCs irrevocably affects the final pancreas size (7). The proliferation of MPCs is accompanied by growth and branching of the pancreatic epithelium into the surrounding mesenchyme. This early phase of pancreas development, also termed primary transition, leads to the first wave of endocrine cell differentiation (8). Some of these early glucagon (Gcg)⁺, but also insulin (Ins)⁺ and Gcg⁺Ins⁺ cells, contribute to the mature islets (5,9). During the secondary transition from E12.5 until birth, the pancreatic epithelium undergoes extensive exocrine and endocrine differentiation (3). A second wave of scattered endocrine progenitors delaminate from the ductal epithelium, coalesce and form, at the end of gestation, the islets of Langerhans. They encompass five major cell types - α , β , δ , PP, ϵ - that produce Gcg, Ins, somatostatin (Sst), pancreatic polypeptide (Ppy), and ghrelin (Ghrl), respectively.

The Vitamin A (VA)-derived all-*trans* RA is a small lipophilic morphogen that regulates gene expression by binding to and activating nuclear RA receptors. During embryogenesis, RA is synthesized in a two-step enzymatic reaction, in which retinol dehydrogenase-10 (Rdh10) first oxidizes VA to retinal (10-12). Several retinal dehydrogenases (Raldhs) then further oxidize retinal to RA (13,14). Previous studies in zebrafish, *Xenopus* and birds have shown an important role of RA signalling in pancreas specification (15-19). In the mouse, overexpression of the dominant-negative RA receptor- α in the pancreas anlagen leads to complete pancreas agenesis, lacking both dorsal and ventral pancreata, suggesting an intrinsic role for RA signalling in MPCs (20). This result contrasts

with *Raldh2* null mutant mice **where** early bud development of the dorsal but not ventral pancreas is impaired (21,22), indicating the existence of a *Raldh2*-independent source of RA that specifies the ventral pancreas anlage. It is not known whether epithelium-derived retinoids contribute to early pancreas organogenesis.

In an *ex vivo* mouse explant system, RA treatment can induce Ins⁺ β -cells from MPCs (20). β -cell differentiation is also stimulated in VA-treated explants, suggesting that an endogenous RA synthesis system might exist in the developing pancreas. *Raldh1* is expressed in the pancreatic epithelium when β -cells normally form, but the identity of the VA-metabolizing enzyme that mediates β -cell differentiation is not known. VA-deprivation and *in vitro* loss-of-function studies support a positive role of retinoids in the regulation of the endocrine mass (23-26). However, nutritional retinoid deficiency influences several tissues simultaneously, and it is impossible to distinguish primary effects in the pancreas from those that are secondarily caused by effects in other tissues. Indeed, the lack of a mammalian genetic model for the **conditional** disruption of VA metabolism ***in vivo*** has so far prevented **the investigation of** the role **and tissues-specific contribution** of RA signals in the differentiation of **pancreatic endocrine cells**.

Using whole embryo and conditional ablation of *Rdh10* in the mouse, we now address the spatial control of retinoid biosynthesis in pancreas organogenesis and cell differentiation. Global loss of the *Rdh10* gene results in a lack of dorsal mesenchyme, failure of the dorsal pancreas to develop, and a smaller ventral pancreas with reduced tubulogenesis. Endoderm-specific deletion of *Rdh10* reduces the size of the dorsal pancreas and the density of early hormone-expressing cells in a RA-dependent manner. **Neurogenin3** (Ngn3)⁺ endocrine progenitors are reduced in both primary and secondary transition, which contributes to the decrease of **endocrine cells and lowered blood glucose levels** in the mutant. Our characterization of marker genes uncovers a key role of *Rdh10* in endocrine cell specification and gives valuable insights into the sources of retinoids during the differentiation of α - and β -cells.

Materials and Methods

Gene targeting and genotyping

Exons 3 and 4 encode amino acids 176-256 including the active site of the Rdh10 enzyme. The conditional ‘floxed’ *Rdh10* allele was generated by inserting a *loxP* site upstream of exon 3 and an *FRT-PGK-neo-FRT-loxP* cassette downstream of exon 4. The *FRT*-flanked neomycin resistance gene under the control of the *PGK* promoter (*FRT-PGK-neo-FRT*) was not excised by Flp recombinase from the ‘floxed’ *Rdh10* allele. Cre-mediated recombination removed exon 3, exon 4 and *FRT-PGK-neo-FRT*, causing a shift of the *Rdh10* open reading frame that led to three aberrant codons followed by a stop codon. ‘Floxed’ *Rdh10* mice were interbred with a modified *Nestin-Cre* transgene, which ubiquitously expresses Cre recombinase early in embryogenesis including the germline (a kind gift from Dr. Werner Müller, University of Manchester, UK) (27). After successful excision of the ‘floxed’ *Rdh10*, *Nestin-Cre* was removed by breeding. Crossing of the *Rdh10*^{+/-} strain gave rise to *Rdh10* knockout (*Rdh10*^{-/-}) embryos. ‘Floxed’ *Rdh10* mice were interbred with *Foxa2*^{Cre} (*Foxa2*^{iCre}) (28) knock-in mice (a kind gift from Dr. Heiko Lickert, Helmholtz Center, Munich, Germany) to obtain an endoderm-specific deletion of the ‘floxed’ *Rdh10* allele. *Foxa2-Cre* does not contain a human growth hormone minigene. The *Rosa26R-lacZ*^{F/+} reporter line (*Gt(ROSA)26Sor*^{tm1Sor}; The Jackson Laboratory) (29) was used to track Cre recombinase activity. The experimental group was comprised of *Rdh10*^{-/-}, *Foxa2*^{Cre/+};*Rdh10*^{F/-} (designated *FRKO*) and *FRKO*;*Rosa26R-lacZ*^{F/+} genotypes. *Foxa2*^{Cre/+};*Rdh10*^{F/-} (designated *FRhet*), *FRhet*;*Rosa26R-lacZ*^{F/+} and control genotypes, including wild type, *Rdh10*^{F/+} and *Foxa2*^{Cre/+};*Rdh10*^{+/+}, exhibited no overt phenotypes and were used as the reference group. Mice and embryos were genotyped by PCR, using genomic DNA from ear or tail tip samples. Primers and conditions for PCR-based genotyping are listed in Supplemental Table 1.

Blood glucose measurement and retinoid rescue experiments

The blood glucose levels in freshly sacrificed postnatal day 7 pups were measured with a handheld glucometer (OneTouch; Lifescan). To rescue the *Rdh10* deficiency phenotype in *FRKO* embryos, all-*trans* retinal (Sigma R2500) and all-*trans* retinoic acid (Sigma R2625) were supplemented to the

maternal diet as described (Supplemental Table 2) (30). Briefly, under red light exposure, stock suspensions were prepared in ethanol at 50 mg/ml for retinal and 5 mg/ml for RA and stored in light-protected glass vials at -20°C. For food paste preparation, retinoid suspensions were diluted in water as 2x stock and mixed 1:1 with powdered food (R36 breeding diet from Lantmännen Lantbruk, Malmö, Sweden). Fresh food paste was administered daily at 8:00 am in clean cages covered with an aluminium foil. A local ethics committee for animal research approved the animal work.

Fixation and histology

For timed pregnancies, the overnight vaginal plug was counted. Embryos until E9.5 (and E11.5 embryos for Ngn3 immunofluorescence) were fixed at 4°C in 4% paraformaldehyde in PBS for 4 hrs. Older embryos were fixed overnight. Following washes in PBS and dehydration, embryos were embedded in paraffin, sectioned at a thickness of 6 µm and stained with hematoxylin-eosin. Alternatively, fixed embryos were incubated overnight at 4°C in 30% sucrose, snap-frozen on dry ice in OCT medium and sectioned at a thickness of 10 µm for *in situ* hybridization and immunofluorescence.

In situ hybridization

In situ hybridization on whole-mount and sectioned embryos was performed as described by (31) and (32), respectively. Digoxigenin-labelled riboprobes were prepared from cDNA plasmids for *Rdh10* (kindly provided by Dr. Pascal Dollé, IGBMC, Illkirch) (33), *Rbp4* (32), and a 2242-bp cDNA encompassing the entire *Raldh2* open reading frame (GenBank/NCBI access. no. BC075704.1 obtained from the I.M.A.G.E. Consortium, www.imageconsortium.org).

Immunofluorescence

For antigen retrieval, the slides with embryo or pancreas sections were boiled in sodium acetate (10 mM, pH 6.0) in the microwave at medium setting two times for 5 minutes. In the case of Ngn3 staining, the antigen retrieval was performed in sodium citrate (10 mM, pH 6.0) at 60°C for 30 minutes. After rinsing three times in PBS, the specimens were blocked with 5% horse serum in PBS

in a wet chamber for 1 hour at room temperature. A mixture of primary antibodies in 5% horse serum and PBS was added and incubated overnight at room temperature. Following rinsing three times in PBS, secondary antibodies in 5% horse serum and PBS were added under light-protection for 2 hours at room temperature. After three PBS rinses, the slides were treated with fluorescence mounting medium (Dako) and allowed to dry for 5 minutes at room temperature. For nuclear staining, DAPI (Sigma, 1:1000) was added to the mounting medium. Antibodies are listed in Supplemental Table 3.

RNA isolation and quantitative PCR

RNA extraction from whole pancreata, reverse transcription, and qPCR were performed as described (34), using 200 ng (E15.5) or 500 ng (E18.5) RNA and 1:100 (E15.5) or 1:200 (E18.5) diluted cDNA. Primer sequences of tested genes are listed in Supplemental Table 4. Gene expression data were normalized to the expression of the internal *Hprt* control gene. If not otherwise indicated, experiments were repeated at least three times, each in triplicate.

Image and statistical analyses

Immunofluorescence was observed, using an Axioplan 2 microscope and Axiovision 4.8 software (Zeiss). The pancreatic area was delineated by hand, and the percentage of pH3⁺, Ngn3⁺, Pax6⁺, Gcg⁺, Ins⁺, Sst⁺-cells was assessed by manually quantifying the cell area or cell number at intervals of 12 μm (for E10.5), 18 μm (E11.5, E12.5), or 30 μm (E14.5, E15.5) throughout the whole pancreas. At E11.5, Ngn3⁺ cells of the whole pancreas were analysed. If not otherwise indicated, statistical measurements were performed using a one-tailed Student's t-test. For E14.5 and E15.5, multiple analysis of variance (MANOVA) was used. Data are presented as mean±standard deviation, using SigmaPlot and Photoshop.

Results

Rdh10 expression in the pancreas

By whole-mount *in situ* hybridization of mouse embryos, we detected tissue-specific *Rdh10* expression as previously reported (10,33) in the hindbrain region, posterior branchial arches, dorsal somites, lateral plate mesoderm and foregut endoderm at E9.0 (Figure 1A,A') and also in the fronto-nasal region, eye, and ear anlagen at E10.5 (Figure 1B). Notably, specific *Rdh10* signals were observed in the pancreas region (arrowheads in Figure 1A',B'). A sense *Rdh10* probe used as background control did not give any signal (Figure 1C,D).

In situ hybridization of sectioned E9.5 embryos revealed *Rdh10* expression in the posterior foregut epithelium (Figure 1F) at the level where antiserum against the transcription factor Pdx1 specifically demarcates the dorsal and ventral pancreas primordia (Figure 1E) (35). *Rdh10* was also expressed in the surrounding mesenchyme, including the *Raldh2*-positive dorsal mesenchyme (Figure 1F,G) (21,22). At E11.5, combined *in situ* hybridization and immunofluorescence revealed abundant *Rdh10* expression in the mesenchyme and partial co-localization with early Gcg⁺ cells of the dorsal pancreatic bud (Figure 1H). *Rdh10* transcripts were detected in the ventral mesenchyme and at very low levels in the ventral pancreatic epithelium (Supplemental Figure 1A-B'). Distinct *Rdh10* expression was observed in the liver at E15.5 and in amylase (Amy)⁺ pancreatic acinar cells at E15.5 and E18.5 (Figure 1I,J; Supplemental Figure 1C). The specificity of the *Rdh10 in situ* hybridization signals was supported by an overlap with previously described expression domains in the spleen, stomach, and intestine (Figure 1I; Supplemental Figure 1C) (33) and severe signal reduction in pancreatic acinar cells after conditional *Rdh10* mutation (Supplemental Figure 1D,E). qPCR analysis indicated that *Rdh10* mRNA levels in the pancreas of wild type embryos increased from E15.5 (Supplemental Figure 1F) to E18.5 (Supplemental Figure 1G). Together, our analyses show new expression domains of *Rdh10* in the developing pancreas and surrounding mesenchyme.

Generation of a conditional knockout model of *Rdh10*

To study the function of *Rdh10* in the mouse, we generated a conditional loss-of-function model, in which exons 3 and 4 of the *Rdh10* gene were excised by Cre-mediated recombination (Supplemental Figure 2A, see Materials and Methods). A similar targeting strategy was previously reported (30). The neomycin resistance (*neo*) gene cassette remained in the absence of Cre recombinase in the *LoxP*-flanked ('floxed') *Rdh10* allele in this study. Using qPCR analysis, we found comparable *Rdh10* transcript levels in pancreatic explants of wild type, *Rdh10*^{F/+} and *Rdh10*^{F/F} littermates at E15.5 (Supplemental Figure 1F), which shows that the promoter of the *neo* gene did not affect *Rdh10* gene expression. We crossed the 'floxed' *Rdh10* allele with a ubiquitously expressed *Nestin*-Cre transgene (27) to generate heterozygous (*Rdh10*^{+/-}) offspring (Supplemental Figure 2B). *Rdh10*^{+/-} mice were indistinguishable from wild type controls (data not shown) but lacked viable homozygous *Rdh10*^{-/-} offspring. The time of embryonic lethality depended on the genetic background (Supplemental Table 5) and varied between E10.5 (C57Bl/6) and E13 (75% NMRI-25% C57Bl/6 mixed strain), in agreement with previously published *Rdh10* knockout models (30,36,37). *Rdh10*^{-/-} embryos exhibited the same craniofacial, forelimb and organ defects (Supplemental Figures 2C-G', 3A-T) that were already described in other *Rdh10* mutants (10,30,36-39), indicating efficient inactivation of *Rdh10*. Hematoxylin and eosin staining at E12.5 confirmed that *Rdh10*^{-/-} mutants had a reduced heart with only one atrium and misaligned ventricles, no lung, a hypoplastic liver, and a small collapsed and medially aligned stomach (Supplemental Figure 3M-T). The septum transversum was also reduced in the absence of *Rdh10* (Supplemental Figure 3O-R). The oesophagus of null mutants appeared to be normal, but no obvious trachea was formed (Supplemental Figure 3Q,R, and data not shown).

Complete inactivation of *Rdh10* causes dorsal pancreas agenesis

Histological analysis showed that in wild type control embryos at E12.5, the dorsal pancreas is located close to the stomach and the ventral pancreas adjacent to the liver (Figure 2A,A'). In *Rdh10*^{-/-} embryos, only a single small pancreatic bud formed (30) and its location near the liver suggested that this structure might be the ventral pancreas (Figure 2B,B'). Indeed, immunofluorescence analysis confirmed that disruption of *Rdh10* caused failure of the dorsal pancreas to develop. At E9.5, control

embryos exhibited a thick, multilayered Pdx⁺ dorsal pancreas anlage (Figure 2C). The transcription factor Islet1 (Isl1) (40) was expressed in a few intermingled Pdx1⁺ cells in the dorsal foregut epithelium and in the adjacent mesenchyme (Figure 2E,E'). *Rdh10*^{-/-} siblings had a thin dorsal foregut epithelium, which consisted of only 1 to 2 cell layers and lacked Pdx1 expression (Figure 2D). In the mutant embryo, Isl1 expression was abundant in the dorsal foregut epithelium, whereas Isl1⁺ dorsal mesenchyme was severely reduced (Figure 2F,F'). Later, the dorsal pancreatic lobe in control embryos contained MPCs that expressed Pdx1, Ptf1a and Nkx6-1 at E10.5 (Supplemental Figure 4C) and also Sox9 at E11.5 (Figure 3A-B). In *Rdh10*^{-/-} littermates, no dorsal pancreas structure with expression of these transcription factors was detected, supporting dorsal pancreas agenesis. Thus, *Rdh10* has a crucial role in dorsal pancreas development likely as a result of impaired dorsal mesenchyme formation.

***Rdh10* knockout leads to hypoplasia of the ventral pancreas**

In *Rdh10*^{-/-} embryos at E9.5, the mesenchyme surrounding the Pdx1⁺ ventral pancreas anlage appeared to be reduced and did not express Isl1 as in wild type control littermates (Figure 2C,D; Supplemental Figure 4A-B'), suggesting a role of *Rdh10* in the formation and patterning of the ventral pancreatic mesenchyme. The distribution of MPCs expressing Pdx1, Ptf1a and Nkx6-1 at E10.5 (Supplementary Figure 4D,E) and also Sox9 at E11.5 (Figure 3C-F) did not differ in the ventral pancreas epithelium of wild type control and *Rdh10*^{-/-} embryos. Furthermore, the ratio of Gcg⁺ cells per pancreas area at E10.5 and E12.5 was not changed between the two genotypes (Figure 3G; Supplemental Figure 4F,G). However, the ventral pancreatic bud in *Rdh10*^{-/-} embryos displayed a consistent half-size reduction compared to control siblings at E10.5, E11.5, and E12.5 (Figure 3H). Interestingly, the relative numbers of phosphorylated Histone3 (pH3)⁺ cells (Figure 3I; Supplemental Figure 4H,I) and TUNEL⁺ cells (data not shown) in the ventral pancreatic epithelium were not different between control and mutant embryos during this period, suggesting normal proliferation and apoptosis rates after *Rdh10* disruption. At E11.5, the ventral pancreatic bud is normally surrounded by a Laminin⁺ basement membrane, whereas Mucin1⁺ apical membranes of inner epithelial cells generate the central microlumen (Figure 3J-J'') (41,42). Epithelial branching is in part triggered by the formation of a

tubular network that arises through fusion of microlumen structures at E12.5 (Figure 3L-L’’’). In *Rdh10*^{-/-} embryos, the Laminin⁺ basement membrane was intact, but the ventral pancreas did not form Mucin1⁺ microlumen at E11.5 (Figure 3K-K’’’) and failed to develop a complex tubular network at E12.5 (Figure 3M-M’’’), suggesting a possible delay in tubulogenesis and branching in accordance with the smaller size of the epithelium. We conclude that *Rdh10* has a crucial role in stimulating the size and morphogenesis of the ventral pancreatic epithelium.

Depletion of *Rdh10* in the endoderm stimulates perinatal mortality, growth retardation and decreased blood glucose levels

The early expression in the posterior foregut prompted us to investigate the role of *Rdh10* in the endoderm. We interbred the conditional ‘floxed’ *Rdh10* allele with the *Foxa2*-Cre knock-in line, which drives Cre recombinase activity in the definitive endoderm from E7.5 as well as the node, notochord and floorplate (28). *Rdh10* expression in the anterior notochord and floorplate (10,33) is distant to the ventral and dorsal pancreas primordia (43) and should therefore not interfere the analysis of *Foxa2*-Cre-driven disruption of the ‘floxed’ *Rdh10* allele in the endoderm. In E18.5 pancreata, *Foxa2*-Cre recombinase reduced *Rdh10* mRNA levels to 55% in *Foxa2*^{Cre/+};*Rdh10*^{F/+} heterozygous (*FRhet*) and 20% in *Foxa2*^{Cre/+};*Rdh10*^{F/-} knockout (*FRKO*) compared to wild type controls (Supplemental Figure 1G). Residual *Rdh10* expression in the *FRKO* pancreas is partially due to the presence of intermingled mesenchyme (44) that is not targeted by the *Foxa2*-Cre recombinase activity. The ratio of *Rdh10*⁺ versus Amy⁺ exocrine pancreatic cells was 50% in the control (*Rdh10*^{F/+}) and 7.25% in the *FRKO* embryos (Figure 1J, Supplemental Figure 1D,E), suggesting that the *Foxa2*-Cre recombinase has an efficiency of 85.5% to eliminate *Rdh10* in targeted cells.

No significant differences were observed between control (wild type, *Rdh10*^{F/+}, *Foxa2*^{Cre/+};*Rdh10*^{F/+}) and *FRhet* mice in their survival (Figure 4A, Supplemental Table S6), weight (Supplemental Figure 5A), blood glucose level (Figure 4E), embryonic visceral organs (compare Supplemental Figure 3M,O,Q,S with Supplemental Figure 6A,C,E,G), pancreas histology (compare Figure 2A,A’ with Supplemental Figure 6I), as well as acinar and hormone gene expression (Supplemental Figure 9). For

this reason and because the transcription factor *Foxa2* plays important roles in the development of gut-derived organs, including the pancreas and endocrine cells (45,46), we compared *FRKO* with, unless otherwise stated, *FRhet* littermates as reference in the following analyses. Endodermal depletion of *Rdh10* did not affect the survival of *FRKO* embryos up to E18.5, but lowered their survival rate to less than 40% at postnatal day 21 (P21) compared to control (*Rdh10^{F/+}*) and *FRhet* siblings (Figure 4A; Supplemental Table 6). The high proportion of dead *FRKO* pups at P0 suggests that partial lethality occurs already around birth (Supplemental Table 6). *FRKO* embryos at E15.5 were the same size as control and *FRhet* littermates (Figure 4B, Supplemental Figure 5A). However, *FRKO* animals were significantly smaller at E18.5 (93%) and at P7, 80% the size of their *FRhet* siblings (Figure 4B,C). They maintained a reduced size as adults (Supplemental Figure 5B), indicating growth retardation in the last days of gestation and first week after birth. Interestingly, *FRKO* pups at P7 had 21% lower blood glucose levels than control (*Foxa2^{Cre/+};Rdh10^{+/+}*) and *FRhet* siblings (Figure 4D), suggesting a role of endodermal *Rdh10* in glucose homeostasis.

Endodermal *Rdh10* contributes to the differentiation of early hormone expressing cells in the dorsal pancreas

To address the underlying cause of the reduced survival rate, growth retardation and misregulated blood glucose levels upon endodermal depletion of *Rdh10*, we first investigated the histology and cell differentiation in mid-gestation embryos. Upon *Foxa2*-Cre-triggered *Rdh10* depletion, the heart, lung, septum transversum, liver, stomach and intestine, as well as both dorsal and ventral pancreatic lobes appeared normal at E12.5 (Supplemental Figure 6B,D,F,H,J). *FRhet* and *FRKO* embryos with an introgressed *Rosa26R-lacZ^{F/+}* reporter (29) showed LacZ reporter expression in *Pdx1⁺* and *Gcg⁺* pancreatic epithelium, but not in surrounding mesenchyme, validating *Foxa2*-Cre recombinase activity in the endoderm-derived epithelium and exclusion from mesodermal mesenchyme (Figure 5A-B''). *FRKO* dorsal and ventral pancreatic buds exhibited normal tubulogenesis (Supplemental Figure 7 and data not shown). Interestingly, the *FRKO* dorsal pancreas was ~40% smaller than wild type control and *FRhet* equivalents (Figure 5A-D,G). Moreover, its number of *Gcg⁺* and *Ins⁺* cells per pancreas area was decreased to ~45% compared to *FRhet* controls (Figure 5A-D,H,I). In contrast,

FRKO did not affect the size and Gcg⁺ cell number of the ventral pancreas (Figure 5J,K). The number of Ins⁺ cells was too low to be quantified in this region. Together, the results show that endodermal *Rdh10* positively regulates the size of the dorsal pancreas and the density of early endocrine cells.

***Rdh10* affects dorsal pancreas and early endocrine development in a RA-dependent manner**

All organ defects previously described in other *Rdh10* mutant embryos can be largely rescued by dietary supplements with retinal and RA (10,30,37-39). To validate that the defects in pancreas and endocrine cell development upon endodermal depletion of *Rdh10* result from reduced endogenous RA levels, we supplemented the diet of pregnant females with exogenous retinoids (Supplemental Table 2). Transplacental administration of 0.4 mg retinal or 0.2 mg RA per gram food each day between E8.5 and the time of analysis at E12.5 rescued the dorsal pancreas size and early endocrine cell numbers in *FRKO* embryos (Figure 5E-I). Administration of retinal and RA to control (*Rdh10*^{F/+}) embryos failed to increase both the dorsal pancreas size and the number of hormone-expressing cells (Supplemental Figure 8A-C), possibly because compensatory feedback mechanisms might suppress higher RA levels *in situ* even if the systemic dose is increased (47). Of note, exogenous retinal and RA treatment neither affected the size nor the Gcg⁺ cell number of the mutant and control (*Rdh10*^{F/+}) ventral pancreas (Figure 5J,K; Supplemental Figure 8D,E). Hence our results suggest that endodermal *Rdh10* contributes to endogenous RA biosynthesis in early pancreas organogenesis and stimulates in a RA-dependent manner dorsal pancreas size and early endocrine cell differentiation.

***Rdh10* is essential for early Ngn3, Pax6, and MafB expression in the dorsal pancreas**

To further elucidate the molecular nature of the defects observed following *Rdh10* depletion, we performed immunofluorescence analysis of key transcription factors that are involved in the first wave of endocrine cell differentiation (Figure 6). Ngn3, Pax6 and MafB are expressed in endocrine progenitors and required for their differentiation towards early Gcg⁺ and Ins⁺ cells (48-50). During the primary transition, Ngn3 protein levels peak at E10.5, and decreases thereafter in the dorsal pancreas (51). We observed that at E11.5, the relative number of Ngn3⁺ cells was reduced by 35% in the *FRKO* compared to the *FRhet* dorsal pancreas, whereas no change was observed in the ventral

pancreas (Figure 6A-C). Hence the reduction of early hormone⁺ cells in the *Rdh10*-deficient dorsal pancreas is not due to a delay in development but, at least in part, resulting from the decreased number of Ngn3⁺ precursors.

Pax6 expressing cells are derived from Ngn3⁺ precursors (48,52), and Pax6 acts upstream of MafB in the specification of Gcg⁺ and Ins⁺ cells (53). Like in *FRhet*, the *FRKO* pancreata at E12.5 exhibited Pax6 and MafB proteins mostly in the nuclei of Gcg⁺ cells, but with a small percentage also in Gcg⁻ endocrine progenitors (Figure 6D-G). The relative numbers of Pax6⁺ and MafB⁺ cells were reduced in the *FRKO* dorsal pancreas. Interestingly, Pax6⁺ cells were equally decreased by ~50% in mutant Gcg⁺ and Gcg⁻ cells (Figure 6H,I), suggesting a reduction of both hormone-expressing and immature endocrine precursor cells. As expected, the proportion of Pax6⁺ and MafB⁺ cells was not significantly altered in the *FRKO* ventral pancreas. The fact that mesenchymal *Rdh10* cannot rescue the reduction of endocrine progenitors in the *FRKO* dorsal pancreas underscores an intrinsic function of *Rdh10* in early MPCs and endocrine cells during the primary transition.

***Rdh10* stimulates hormone expression in late endocrine cells**

We next studied whether *Rdh10* is involved in the regulation of acinar- and endocrine-specific genes during the secondary transition (Figure 7). Quantitative PCR (qPCR) showed a reduction of *Rdh10* transcript levels to 40% at E15.5 and to 25% at E18.5 in extracted pancreata of *FRKO* embryos compared to *FRhet* siblings (Figure 7A). Although *Rdh10* is robustly expressed in acinar cells (Figure 1I,J; Supplemental Figure 1C), the mRNA levels of neither *Amy* at E15.5 nor *Amy* and *Carboxypeptidase1* (*Cpa1*) at E18.5 were altered in the *FRKO* pancreas compared to the *FRhet* littermate and wild type control (Figure 7B; Supplemental Figure 9A). Moreover, the rosette organization of acinar cell clusters appeared normal in *FRKO* pancreata at these stages (Figure 1J; Supplemental Figures 1D, 10A-D), suggesting that intrinsic *Rdh10* does not affect acinar cell differentiation in the developing pancreas.

At E15.5, relative *Gcg* and *Ins* mRNA levels were both reduced by 20% in the *FRKO* compared to the *FRhet* pancreas, whereas *Sst* and *Ghrl* mRNA levels were not affected (Figure 7C). To investigate region-specific differences in hormone expression, we performed immunofluorescence analysis on sectioned embryos, using the portal vein as landmark to segregate the dorsal and ventral pancreata (Supplemental Figure 6K). The *FRKO* dorsal pancreas was ~20% smaller than in *FRhet* controls, while the ventral pancreas did not show a significant size difference (Figure 7E). In agreement with the qPCR data, we found a ~20% decrease in the proportion of *Gcg*⁺ and *Ins*⁺ cells and no change in the relative number of *Sst*⁺ cells in the mutant dorsal pancreas, whereas the abundance of these hormone-expressing cells was not altered in the mutant ventral pancreas (Figure 7F-H; Supplemental Figure 10A,B). At E18.5, the *FRKO* pancreas exhibited a significant decrease of *Gcg*, *Ins*, *Sst*, and *Ppy*, but no change of *Ghrl* mRNA levels compared to the *FRhet* sibling and wild type control (Figure 7D; Supplemental Figure 9B). The results indicate a supportive role of *Rdh10* in the formation of α -, β -, δ -, and PP-cells.

***Rdh10* restricts the expression of *Rbp4* in endocrine cells**

Expression of *Rbp4* encoding the retinol-binding protein-4 has been reported in most *Gcg*⁺ and *Ins*⁺ cells at E15.5 and in a small fraction of *Ins*⁺, *Gcg*⁺, and *Sst*⁺ cells at E18.5 (32). *In situ* hybridization showed *Rbp4* transcripts in both *Gcg*⁺ and *Gcg*⁻ cells but apparently not in rosette-like acini in E15.5 dorsal pancreata of both genotypes (Supplemental Figure 10C,D). By qPCR, we detected ~40% higher *Rbp4* mRNA levels in the *FRKO* compared to *FRhet* pancreas at E18.5 (Figure 8A). The results suggest feedback regulation of a major retinol storage component in the pancreas and might explain the relatively mild endocrine cell differentiation phenotype in the *FRKO* pancreas.

***Rdh10* controls the number of *Ngn3*-positive cells during the secondary transition**

To further investigate whether *Rdh10* is required for the specification of definitive endocrine cells, we focused on the progenitor cell marker *Ngn3*, which is essential for the development of all endocrine cells (5,48). During secondary transition, *Ngn3*⁺ cells in the pancreatic trunk epithelium undergo a

progression from initially uncommitted but endocrine-biased cells with low levels of Ngn3 protein (Ngn3^{LO}) towards high Ngn3-expressing (Ngn3^{HI}) endocrine progenitors that are irreversibly committed and allocated to a single endocrine cell lineage (Figure 8B) (54,55). Although qPCR analysis did not show a significant change in *Ngn3* mRNA levels between *FRKO* and *FRhet* control pancreata at E15.5 (Supplemental Figure 10E), the number of Ngn3^{HI} cells in the *FRKO* dorsal pancreas was decreased and Ngn3^{LO} cells in the mutant ventral pancreas elevated by each 25% at E14.5 (Figure 8C,D). Thus, *Rdh10* might enhance the generation of α - and β -cells during secondary transition by stimulating the production of committed Ngn3^{HI} endocrine progenitors specifically in the dorsal pancreas.

***Rdh10* regulates the islet cell differentiation program**

During the secondary transition, Pax6-expressing pan-endocrine cells are, with a few exceptions, non-overlapping with Ngn3⁺ cells in *FRhet* and *FRKO* embryos (Figure 8B'-C'') (52). At E14.5, the relative amount of Pax6⁺ cells in neither the dorsal nor the ventral pancreas was significantly different between both genotypes (Figure 8E). Transcription factors with important functions in distinct endocrine cell lineages encompass the α -cell specific *Arx* (56), the β -cell specific *NeuroD* (57), *Nkx6-1* (58), *MafA* (32), *Pax4* (59) and the α/β -specific *MafB* (50). A comparison of both genotypes by qPCR did not show different mRNA levels of *MafB* at E15.5 and E18.5 nor of *NeuroD* at E18.5 (Figure 8F; Supplemental Figure 10E). However, we observed downregulation of *Arx* (20%), *Nkx6-1* (20%), and *MafA* (35%) mRNAs in the *FRKO* pancreas at E18.5 (Figure 8F). In contrast, both *Pax4* and *Pax6* mRNA levels were increased by each 60%, suggesting an accumulation of endocrine precursors in the mutant pancreas. The moderate decrease of *Arx* and *Nkx6-1* expression might be due to the decline of α - and β -cells, whereas the more robust downregulation of *MafA* as well as upregulation of *Pax4* and *Pax6* expression indicate abnormal endocrine cell development. The increased *Pax6* mRNA levels in *FRKO* pancreata at the end of gestation prompted us to analyze the expression of *GLUT2*, which is positively regulated by Pax6 (60) and encoding an Ins-responsive glucose transporter responsible for the glucose uptake specifically in β -cells. As expected, *Rdh10*

depletion caused a ~20% increase in the *GLUT2* mRNA level at E18.5 (Figure 8G). Together, endodermal *Rdh10* exerts differential regulation of key endocrine transcription factors, supporting functions at multiple steps of the islet cell differentiation program.

Discussion

Although *Rdh10* has been inactivated previously in the mouse (10,30,36,37,39), its role in pancreas development has not been studied yet. Here we report the complete and conditional disruption of the *Rdh10* gene and the consequences on pancreas organogenesis, endocrine cell lineage and glucose homeostasis. We suggest that the endoderm is a critical source of retinoid biosynthesis in early and late pancreatic endocrine cell differentiation.

We previously demonstrated at the late gastrula stage in *Xenopus* embryos that *Rdh10* and *Raldh2* expression partially overlaps in the anterior trunk mesoderm and is essential for patterning the anteroposterior axis of the overlying neural plate (11). Co-expression of murine *Rdh10* (10,33) and *Raldh2* (21,22) in the anterior trunk mesoderm led us hypothesize that both enzymes might also cooperate in specifying the dorsal pancreas anlage in the underlying foregut endoderm. In the mouse embryo, we found that *Rdh10* is expressed in the posterior foregut epithelium at the prospective pancreas level and overlaps with *Raldh2* in the dorsal mesenchyme. The circulation supplies VA (14), and the dorsal aorta is essential for dorsal pancreas formation and endocrine cell differentiation (65). We propose a model (Figure 9A), in which the dorsal aorta delivers VA that is then metabolized by *Rdh10* in the adjacent dorsal foregut epithelium and overlying mesenchyme. *Rdh10* thereby provides mesenchymal *Raldh2* with retinal and establishes a localized source of bioactive RA. RA in turn diffuses back into the foregut epithelium and acts as a paracrine signal to promote both dorsal pancreas development and early endocrine cell differentiation. In agreement with this model, we found that complete disruption of *Rdh10* caused a lack of *Pdx1* expression in the dorsal foregut and a failure to form a dorsal pancreatic bud. Nevertheless, pancreatic cell fate might have been committed, because *Isl1* expression was retained in the dorsal foregut epithelium of *Rdh10*^{-/-} embryos. A similar

phenotype has been described for *Raldh2*^{-/-} embryos (21,22), supporting a functional collaboration between Rdh10 and Raldh2 in localized RA production during dorsal pancreas organogenesis. Endodermal depletion of Rdh10 caused a reduction of the dorsal pancreas bud and a decline in the relative number of early Gcg⁺ and Ins⁺ cells. This phenotype was rescued by dietary retinal and RA supplementation, showing for the first time that epithelium-derived retinoids are important for early pancreas organogenesis. The decreased number of endocrine progenitors expressing Ngn3, Pax6 and MafB in the *FRKO* dorsal pancreas suggests that endodermal Rdh10 stimulates the differentiation of early Gcg⁺ and Ins⁺ cells through activation of these transcription factors. Thus, Rdh10 exerts an intrinsic role in the early endocrine cell differentiation program of the dorsal pancreas. The observation that *FRKO* did not fully mimic the complete knockout phenotype indicates a mixed contribution of both mesenchymal and epithelial Rdh10 to dorsal pancreas development.

Signals from the cardiac mesoderm and septum transversum mesenchyme affect region-specific organogenesis in the ventral foregut endoderm, including the liver and ventral pancreas (61,62). Our histological analysis shows that the heart and septum transversum are hypoplastic in *Rdh10*^{-/-} mutants, but apparently normal in *FRKO* embryos, raising the possibility that Rdh10 might promote liver and ventral pancreas development non-cell autonomously through influencing key factors in these mesodermal signaling centers. Consistent with abundant expression of *Rdh10* in the ventral pancreas anlage and surrounding mesenchyme, we observed hypoplasia and reduced tubulogenesis in the ventral pancreas of *Rdh10*^{-/-} embryos. Endodermal depletion of Rdh10 in *FRKO* embryos did not affect the size and shape of the ventral pancreatic epithelium, supporting the idea that the mesenchyme is the primary site of Rdh10 function in ventral pancreas development.

The mesenchyme promotes the growth and subsequent branching morphogenesis of the pancreatic epithelium notably through the secretion of fibroblast growth factor 10 (Fgf10) (44,63). However, several observations argue against an involvement of Fgf10 as mediator of RA signals in pancreogenesis. In *Fgf10*^{-/-} embryos, the pancreatic mesenchyme develops normally and the dorsal pancreatic bud initially forms (63). In contrast, the cytoarchitecture and Isl expression of the dorsal

mesenchyme is impaired and the dorsal pancreatic endoderm fails to expand in *Raldh2*^{-/-} (21) and *Rdh10*^{-/-} embryos. Lowered cell proliferation accounts for the reduced pancreas size in the absence of Fgf10 (63), while proliferation is not decreased in the ventral pancreatic bud of *Rdh10*^{-/-} embryos. In addition, the expression of Sox9, which forms a feed-forward loop with Fgf10 and its cognate Fgf receptor 2b (64), was not reduced in the MPCs of *Rdh10*^{-/-} embryos, which further excludes Fgf10 as the mediator of RA signals in pancreas organogenesis.

It could be argued that the effects on endocrine cell differentiation in *FRKO* embryos might result from mispatterning of the early endoderm. However, β -cell differentiation is decreased in rat embryos that are deprived of VA after the pancreas has already been specified (23) and in isolated human fetal islet epithelial cells upon pharmacological and siRNA-mediated inhibition of RALDH1 (26), supporting a distinct function of RA in definitive endocrine cell differentiation. During secondary transition, *Raldh1* (20) and *Rdh10* are co-expressed in the acinar cells, whereas *Rbp4* encoding the soluble retinol-binding protein-4 is expressed in endocrine cells (32). We suggest that following the release of VA from pancreatic blood vessels the endocrine and exocrine compartments orchestrate a feedback-regulated directional retinoid flow that generates a localized RA source within the pancreas epithelium (Figure 9B). *Rbp4* secreted by endocrine cells binds and accumulates VA, which in turn is metabolized by *Rdh10* and *Raldh1* in flanking acinar cells. RA then is delivered back to endocrine cells to promote their differentiation. Thus *Rdh10* might be the elusive VA-metabolizing enzyme that cooperates with *Raldh1* to stimulate β -cell differentiation upon treatment of pancreatic explants with VA (20). In support of this conclusion, *FRKO* embryos displayed a reduction of α - and β -cells in the dorsal pancreas at E15.5. A significant decline of *Gcg*, *Ins*, *Sst*, and *PP* expression at E18.5 emphasize an intrinsic requirement of *Rdh10* for optimal production of islet cells in the pancreas epithelium. The relatively mild reduction of the endocrine mass upon *FRKO* might be due to a rescue by residual *Rdh10* in the mesenchyme and negative feedback regulation. In agreement with a previous report that RA treatment reduces the *Rbp4* serum concentration in mice (66), we found that epithelial *Rdh10*

deficiency caused upregulation of pancreatic *Rbp4* expression, supporting a possible compensation through feedback control by RA signals.

A recent study in the mouse (67) showed that genetically induced hypoplasia of the pancreatic exocrine tissue causes fewer Ngn3⁺ endocrine precursors and β -cells at E14.5 as well as impaired glucose homeostasis, suggesting that an unknown and important factor in the exocrine tissue regulates proper endocrine cell development and function. *FRKO* mice exhibited a decrease of cells with high Ngn3 expression in the dorsal pancreas at E14.5 and lowered blood glucose levels at P7, supporting that a reduced progenitor pool might account for the decreased number of definitive endocrine cells and lowered glucose homeostasis. In a gain-of-function study, exogenous RA promoted *Ngn3* expression and β -cell differentiation in an *ex vivo* pancreas explant system (20). In contrast, reduction of *Ngn3*, *Gcg*, and *Ins* expression was reported in *RAR β* -knockout mouse embryonic stem cells that were subjected in the petri dish to a pancreatic islet differentiation protocol (25). Hence our loss-of-function data in the embryo support previous *in vitro* experiments and suggest an important role of exocrine cell-derived RA signals *in vivo* in the initiation of definitive islet cell differentiation.

After Pax4 has specified β -cell fate around E13.5-E15.5, its expression normally declines towards the end of gestation (59,68). *Ins* expression is downregulated by Pax4 (69,70) and upregulated by MafA (71). Overexpression of Pax4 and marked decrease of MafA expression in the *FRKO* pancreas at E18.5 suggests that the β -cell lineage might be arrested in a progenitor stage. Thus, we suggest that Rdh10 might promote terminal differentiation of β -cells and *Ins* production by activating MafA and repressing Pax4 expression. This is the first demonstration *in vivo* that endogenously produced retinoids are required for endocrine cell differentiation and the generation of *Ins*-producing β -cells in the developing embryo. A better understanding of the spatio-temporal control of RA signalling in the mouse pancreas facilitates the development of 3D-organ culture to efficiently generate functional β -cells for stem cell-based treatments of diabetes. In present human embryonic stem cell protocols, RA is added early to promote the conversion of definitive endoderm to pancreatic precursors (e.g. 72).

Our identification of defects in the initiation and terminal differentiation of islet cells upon endodermal knockout of *Rdh10* raises the possibility that modulation of RA signalling in a later phase of the differentiation protocol might further boost the efficiency of β -cell differentiation.

Acknowledgements

We thank Drs. Werner Müller and Heiko Lickert for mice, Dr. Pascal Dollé for the *Rdh10* plasmid, and Dr. Fong Chen Pan, Dr. Oliver Wessely, and Linda Wei for discussion and comments on the manuscript. We are grateful to Dr. Emad Ahmed, and Karina Steinkogler for mouse strain maintenance and genotyping.

Author contributions

I. Arregi, M.C. and E.M.P. designed research; L.M. designed the ‘floxed’ *Rdh10* allele; I. Arregi, M.C., D.I., J.S., N.G., J.K.J., T.S. and E.M.P performed experiments; I. Arregi, M.C., D.I., J.S., J.K.J., T.S., M.M., H.S., I. Artner, and E.M.P. analyzed data; I. Arregi, M.C. and E.M.P. wrote the paper.

References

1. Pan FC, Wright C. (2011). Pancreas organogenesis: from bud to plexus to gland. *Dev. Dyn.* 240:530-565.
2. Mastracci TL, Sussel L. (2012). The endocrine pancreas: insights into development, differentiation, and diabetes. *Wiley Interdiscip. Rev. Dev. Biol.* 1:609-628.
3. Shih HP, Wang A, Sander M. (2013). Pancreas organogenesis: from lineage determination to morphogenesis. *Annu. Rev. Cell Dev. Biol.* 29:81-105.
4. Jørgensen MC, Ahnfelt-Rønne J, Hald, J, Madsen, OD, Serup, P, Hecksher-Sørensen J. (2007). An illustrated review of early pancreas development in the mouse. *Endocr. Rev.* 28:685-705.
5. Gu G, Dubauskaite J, Melton, DA. (2002). Direct evidence for the pancreatic lineage: NGN3+ cells are islet progenitors and are distinct from duct progenitors. *Development* 129:2447-2557.
6. Zhou Q, Law AC, Rajagopal J, Anderson WJ, Gray PA, Melton DA. (2007). A multipotent progenitor domain guides pancreatic organogenesis. *Dev. Cell.* 13:103-114.
7. Stanger BZ, Tanaka AJ, Melton DA. (2007). Organ size is limited by the number of embryonic progenitor cells in the pancreas but not the liver. *Nature* 445:886-891.

8. Pictet RL, Clark WR, Williams RH, Rutter WJ. (1972). An ultrastructural analysis of the developing embryonic pancreas. *Dev. Biol.* 29:436-467.
9. Herrera PL. (2000). Adult insulin- and glucagon-producing cells differentiate from two independent cell lineages. *Development* 127:2317-2322.
10. Sandell LL, Sanderson BW, Moiseyev G, Johnson T, Mushegian A, Young K, Rey JP, Ma JX, Staehling-Hampton K, Trainor PA. (2007). RDH10 is essential for synthesis of embryonic retinoic acid and is required for limb, craniofacial, and organ development. *Genes Dev.* 21:1113-1124.
11. Strate I, Min TH, Iliev D, Pera, EM. (2009). Retinol dehydrogenase 10 is a feedback regulator of retinoic acid signalling during axis formation and patterning of the central nervous system. *Development* 136:461-472.
12. Feng L, Hernandez RE, Waxman JS, Yelon D, Moens CB. (2010). Dhhrs3a regulates retinoic acid biosynthesis through a feedback inhibition mechanism. *Dev. Biol.* 338:1-14.
13. Duester G. (2008). Retinoic acid synthesis and signaling during early organogenesis. *Cell* 134, 921-931.
14. Rhinn M, Dollé P. (2012). Retinoic acid signalling during development. *Development* 139:843-858.
15. Stafford D, Prince VE. (2002). Retinoic acid signaling is required for a critical early step in zebrafish pancreatic development. *Curr. Biol.* 12:1215-1220.
16. Chen Y, Pan FC, Brandes N, Afelik S, Sölter M, Pieler T. (2004). Retinoic acid signaling is essential for pancreas development and promotes endocrine at the expense of exocrine cell differentiation in *Xenopus*. *Dev. Biol.* 271:144-160.
17. Stafford D, Hornbruch A, Mueller PR, Prince VE. (2004). A conserved role for retinoid signaling in vertebrate pancreas development. *Dev Genes Evol.* 214:432-441.
18. Pan FC, Chen Y, Bayha E, Pieler T. (2007). Retinoic acid-mediated patterning of the pre-pancreatic endoderm in *Xenopus* operates via direct and indirect mechanisms. *Mech. Dev.* 124:518-531.
19. Bayha E, Jørgensen MC, Serup P, Grapin-Botton A. (2009). Retinoic acid signaling organizes endodermal organ specification along the entire antero-posterior axis. *PLoS One.* 2009 Jun 10;4(6):e5845. doi: 10.1371/journal.pone.0005845.
20. Öström M, Löffler KA, Edfalk S, Selander L, Dahl U, Ricordi C, Jeon J, Correa-Medina M, Diez J, Edlund H. (2008). Retinoic Acid Promotes the Generation of Pancreatic Endocrine Progenitor Cells and Their Further Differentiation into β -Cells. *PLoS ONE* 3(7): e2841. doi:10.1371/journal.pone.0002841.
21. Martín M, Gallego-Llamas J, Ribes V, Keding M, Niederreither K, Chambon P, Dollé P, Gradwohl G. (2005). Dorsal pancreas agenesis in retinoic acid-deficient *Raldh2* mutant mice. *Dev. Biol.* 284:399-411.
22. Molotkov A, Molotkova N, Duester G. (2005). Retinoic acid generated by *Raldh2* in mesoderm is required for mouse dorsal endodermal pancreas development. *Dev. Dyn.* 232:950-957.
23. Matthews KA, Rhoten WB, Driscoll HK, Chertow BS. (2004). Vitamin A deficiency impairs fetal islet development and causes subsequent glucose intolerance in adult rats. *J. Nutr.* 134:1958-1963.

24. Trasino SE, Benoit YD, Gudas LJ. (2015). Vitamin A deficiency causes hyperglycemia and loss of pancreatic β -cell mass. *J. Biol. Chem.* 290:1456-1473.
25. Pérez RJ, Benoit YD, Gudas LJ. (2013). Deletion of retinoic acid receptor β (RAR β) impairs pancreatic endocrine differentiation. *Exp. Cell Res.* 319:2196-2204.
26. Li J, Feng ZC, Yeung FS, Wong MR, Oakie A, Fellows GF, Goodyer CG, Hess DA, Wang R. (2014). Aldehyde dehydrogenase 1 activity in the developing human pancreas modulates retinoic acid signalling in mediating islet differentiation and survival. *Diabetologia* 57:754-764.
27. Betz UA, Vosshenrich CA, Rajewsky K, Müller W. (1996). Bypass of lethality with mosaic mice generated by Cre-loxP-mediated recombination. *Curr. Biol.* 6:1307-1316.
28. Uetzmänn L, Burtcher I, Lickert H. (2008). A mouse line expressing Foxa2-driven Cre recombinase in node, notochord, floorplate, and endoderm. *Genesis* 46:515-522.
29. Soriano P. (1999). Generalized lacZ expression with the ROSA26 Cre reporter strain. *Nat. Genet.* 21:70-71.
30. Rhinn M, Schuhbaur B, Niederreither K, Dollé P. (2011). Involvement of retinol dehydrogenase 10 in embryonic patterning and rescue of its loss of function by maternal retinaldehyde treatment. *Proc. Natl. Acad. Sci U S A.* 108:16687-16692.
31. Conlon RA, Rossant J. (1992). Exogenous retinoic acid rapidly induces anterior ectopic expression of murine Hox-2 genes in vivo. *Development* 116:357-368.
32. Artner I, Hang Y, Mazur M, Yamamoto T, Guo M, Lindner J, Magnuson MA, Stein R. (2010). MafA and MafB regulate genes critical to beta-cells in a unique temporal manner. *Diabetes* 59:2530-2539.
33. Cammas L, Romand R, Fraulob V, Mura C, Dollé P. (2007). Expression of the murine retinol dehydrogenase 10 (Rdh10) gene correlates with many sites of retinoid signalling during embryogenesis and organ differentiation. *Dev. Dyn.* 236:2899-2908.
34. Mazur MA, Winkler M, Ganic E, Colberg JK, Johansson JK, Bennet H, Fex M, Nuber UA, Artner I. (2013). Microphthalmia transcription factor regulates pancreatic β -cell function. *Diabetes* 62:2834-2842.
35. Guz Y, Montminy MR, Stein R, Leonard J, Gamer LW, Wright CV, Teitelman G. (1995). Expression of murine STF-1, a putative insulin gene transcription factor, in beta cells of pancreas, duodenal epithelium and pancreatic exocrine and endocrine progenitors during ontogeny. *Development* 121:11-18.
36. Sandell LL, Lynn ML, Inman KE, McDowell W, Trainor PA. (2012). RDH10 oxidation of Vitamin A is a critical control step in synthesis of retinoic acid during mouse embryogenesis. *PLoS One.* 7(2):e30698. doi: 10.1371/journal.pone.0030698.
37. Chatzi C, Cunningham TJ, Duester G. (2013). Investigation of retinoic acid function during embryonic brain development using retinaldehyde-rescued Rdh10 knockout mice. *Dev. Dyn.* 242:1056-1065.
38. Farjo KM, Moiseyev G, Nikolaeva O, Sandell LL, Trainor PA, Ma JX. (2011). RDH10 is the primary enzyme responsible for the first step of embryonic Vitamin A metabolism and retinoic acid synthesis. *Dev. Biol.* 357:347-355.

39. Ashique M, May SR, Kane MA, Folias AE, Phamluong K, Choe Y, Napoli JL, Peterson, AS. (2012). Morphological defects in a novel *Rdh10* mutant that has reduced retinoic acid biosynthesis and signaling. *Genesis* 50:415-423.
40. Ahlgren U, Pfaff SL, Jessell TM, Edlund T, Edlund H. (1997). Independent requirement for *ISL1* in formation of pancreatic mesenchyme and islet cells. *Nature* 385:257-260.
41. Kesavan G, Sand FW, Greiner TU, Johansson JK, Kobberup S, Wu X, Brakebusch C, Semb H. (2009). *Cdc42*-mediated tubulogenesis controls cell specification. *Cell* 139:791-801.
42. Villaseñor A, Chong DC, Henkemeyer M, Cleaver O. (2010). Epithelial dynamics of pancreatic branching morphogenesis. *Development* 137:4295-4305.
43. Miki R, Yoshida T, Murata K, Oki S, Kume K, Kume S. (2012). Fate maps of ventral and dorsal pancreatic progenitor cells in early somite stage mouse embryos. *Mech Dev.* 128:597-609.
44. Landsman L, Nijagal A, Whitchurch TJ, Vanderlaan RL, Zimmer WE, Mackenzie TC, Hebrok M. (2011). Pancreatic mesenchyme regulates epithelial organogenesis throughout development. *PLoS Biol.* 9(9):e1001143. doi: 10.1371/journal.pbio.1001143.
45. Lee CS, Sund NJ, Behr R, , Kaestner KH. (2005). *Foxa2* is required for the differentiation of pancreatic alpha-cells. *Dev. Biol.* 278:484-495.
46. Gao N, LeLay J, Vatamaniuk MZ, Rieck S, Friedman JR, Kaestner KH. (2008). Dynamic regulation of *Pdx1* enhancers by *Foxa1* and *Foxa2* is essential for pancreas development. *Genes Dev.* 22:3435-3448.
47. Lee LM, Leung CY, Tang WW, Choi HL, Leung YC, McCaffery PJ, Wang CC, Woolf AS, Shum AS. (2012). A paradoxical teratogenic mechanism for retinoic acid. *Proc Natl Acad Sci U S A.* 109:13668-13673.
48. Gradwohl G, Dierich A, LeMeur M, Guillemot F. (2000). *neurogenin3* is required for the development of the four endocrine cell lineages of the pancreas. *Proc. Natl. Acad. Sci. U S A* 97:1607-1611.
49. Sander M, Neubüser A, Kalamaras J, Ee HC, Martin GR, German MS. (1997). Genetic analysis reveals that *PAX6* is required for normal transcription of pancreatic hormone genes and islet development. *Genes Dev.* 11:1662-1673.
50. Artner I, Blanchi B, Raum JC, Guo M, Kaneko T, Cordes S, Sieweke M, Stein R. (2007). *MafB* is required for islet beta cell maturation. *Proc. Natl. Acad. Sci. U S A* 104:3853-3858.
51. Villaseñor A, Chong DC, Cleaver O. (2008). Biphasic *Ngn3* expression in the developing pancreas. *Dev Dyn.* 237:3270-3279.
52. Jensen J, Heller RS, Funder-Nielsen T, Pedersen EE, Lindsell C, Weinmaster G, Madsen O D, Serup P. (2000). Independent development of pancreatic alpha- and beta-cells from *neurogenin3*-expressing precursors: a role for the notch pathway in repression of premature differentiation. *Diabetes* 49:163-176.
53. Nishimura W, Rowan S, Salameh T, Maas RL, Bonner-Weir S, Sell SM, Sharma A. (2008). Preferential reduction of beta cells derived from *Pax6-MafB* pathway in *MafB* deficient mice. *Dev. Biol.* 314:443-456.

54. Desgraz R, Herrera PL. (2009). Pancreatic neurogenin 3-expressing cells are unipotent islet precursors. *Development* 136, 3567-3574.
55. Wang S, Yan J, Anderson DA, Xu Y, Kanal MC, Cao Z, Wright CV, Gu G. (2010). Neurog3 gene dosage regulates allocation of endocrine and exocrine cell fates in the developing mouse pancreas. *Dev. Biol.* 339, 26-37.
56. Collombat P, Mansouri A, Hecksher-Sorensen J, Serup P, Krull J, Gradwohl G, Gruss P. (2003). Opposing actions of Arx and Pax4 in endocrine pancreas development. *Genes Dev.* 17:2591-2603.
57. Naya FJ, Huang HP, Qiu Y, Mutoh H, DeMayo FJ, Leiter AB, Tsai MJ. (1997). Diabetes, defective pancreatic morphogenesis, and abnormal enteroendocrine differentiation in BETA2/neuroD-deficient mice. *Genes Dev.* 11:2323-2334.
58. Sander M, Sussel L, Connors J, Scheel D, Kalamaras J, Dela Cruz F, Schwitzgebel V, Hayes-Jordan A, German M. (2000). Homeobox gene Nkx6.1 lies downstream of Nkx2.2 in the major pathway of beta-cell formation in the pancreas. *Development* 127:5533-5540.
59. Sosa-Pineda B, Chowdhury K, Torres M, Oliver G, Gruss P. (1997). The Pax4 gene is essential for differentiation of insulin-producing beta cells in the mammalian pancreas. *Nature* 386:399-402.
60. Ashery-Padan R, Zhou X, Marquardt T, Herrera P, Toubé L, Berry A, Gruss P. (2004). Conditional inactivation of Pax6 in the pancreas causes early onset of diabetes. *Dev. Biol.* 269:479-488.
61. Deutsch G, Jung J, Zheng M, Lórá J, Zaret KS. (2001). A bipotential precursor population for pancreas and liver within the embryonic endoderm. *Development* 128:871-881.
62. Saito Y, Kojima T, Takahashi N. (2013). The septum transversum mesenchyme induces gall bladder development. *Biol. Open* 2:779-788.
63. Bhushan A, Itoh N, Kato S, Thiery JP, Czernichow P, Bellusci S, Scharfmann R. (2001). Fgf10 is essential for maintaining the proliferative capacity of epithelial progenitor cells during early pancreatic organogenesis. *Development* 128:5109-5117.
64. Seymour PA, Shih HP, Patel NA, Freude KK, Xie R, Lim CJ, Sander M. (2012). A Sox9/Fgf feed-forward loop maintains pancreatic organ identity. *Development* 139:3363-3372.
65. Lammert E, Cleaver O, Melton D. (2001). Induction of pancreatic differentiation by signals from blood vessels. *Science* 294:564-567.
66. Manolescu DC, Sima A, Bhat PV. (2010). All-trans retinoic acid lowers serum retinol-binding protein 4 concentrations and increases insulin sensitivity in diabetic mice. *J. Nutr.* 140:311-316.
67. Kodama S, Nakano Y, Hirata K, Furuyama K, Horiguchi M, Kuhara T, Masui T, Kawaguchi M, Gannon M, Wright CV, Uemoto S, Kawaguchi Y. (2016). Diabetes Caused by Elastase-Cre-Mediated Pdx1 Inactivation in Mice. *Sci. Rep.* 6:21211.
68. Wang J, Elghazi L, Parker SE, Kizilocak H, Asano M, Sussel L, Sosa-Pineda B. (2004). The concerted activities of Pax4 and Nkx2.2 are essential to initiate pancreatic beta-cell differentiation. *Dev. Biol.* 266:178-189.
69. Smith S B, Ee HC, Connors JR, German MS. (1999). Paired-homeodomain transcription factor PAX4 acts as a transcriptional repressor in early pancreatic development. *Mol. Cell Biol.* 19:8272-8280.

- 813
814 70. Campbell SC, Cragg H, Elrick LJ, Macfarlane WM, Shennan KI, Docherty K. (1999). Inhibitory
815 effect of pax4 on the human insulin and islet amyloid polypeptide (IAPP) promoters. FEBS Lett.
816 463:53-57.
817
818 71. Artner I, Hang Y, Guo M, Gu G, Stein R. (2008). MafA is a dedicated activator of the insulin
819 gene in vivo. J. Endocrinol. 198:271-279.
820
821 72. D'Amour KA, Bang AG, Eliazer S, Kelly OG, Agulnick AD, Smart NG, Moorman MA, Kroon E,
822 Carpenter MK, Baetge EE. (2006). Production of pancreatic hormone-expressing endocrine cells from
823 human embryonic stem cells. Nat. Biotechnol. 24:1392-1401.
824

Figure legends

Figure 1. *Rdh10* gene expression during mouse pancreas development

(A-D) Whole-mount *in situ* hybridization of E9.0 and E10.5 embryos. Magnification (A', B') identifies *Rdh10* transcripts in the pancreas regions (arrowheads). No signal can be seen with an *Rdh10* sense RNA control (C,D).

(E) Transversal section of posterior foregut region at E9.5. Immunofluorescence analysis shows Pdx1 expression in the dorsal and ventral pancreas primordia.

(F) *In situ* hybridization identifies *Rdh10* transcripts in the posterior foregut and surrounding mesenchyme.

(G) *Raldh2* transcripts are enriched in the dorsal mesenchyme.

(H) Section of E11.5 embryo after combined *in situ* hybridization and immunofluorescence analysis. Striped line demarcates dorsal pancreas epithelium that is surrounded by *Rdh10*⁺ mesenchyme. Framed area shows *Rdh10* gene expression in Gcg⁺ cell cluster (arrowhead).

(I) Section of E15.5 dorsal pancreas. *Rdh10* transcripts overlap with Amy⁺ exocrine cells (arrow).

(J) Section of E18.5 pancreas. *Rdh10* transcripts are abundant in Amy⁺ exocrine cells (arrow) adjacent to Gcg⁺ α -cell-containing islets of Langerhans.

b, branchial arch; dm, dorsal mesenchyme; dp, dorsal pancreas; ds, dorsal somite; ea, ear; ey, eye; fg, foregut; fl, forelimb; fn, frontonasal region; hb, hindbrain; he, heart; in, intestine; is, islet of Langerhans; lpm, lateral plate mesoderm; sp, spleen; st, stomach; vp, ventral pancreas. Scale bars are 50 μ m.

Figure 2. Disruption of the *Rdh10* gene locus causes dorsal pancreas agenesis

(A-B') Transversal sections of E12.5 embryos after hematoxylin and eosin staining. Dotted lines show the dorsal and ventral pancreas in the wild type control and a hypoplastic ventral pancreas in the *Rdh10*^{-/-} embryo.

(C,D) Immunohistochemistry with anti-Pdx1 antibody in transversal sections of embryos at E9.5. The wild type control has dorsal and ventral pancreas rudiments (C). In the *Rdh10* mutant, Pdx1 immunoreactivity is present in the prospective ventral pancreas but absent in the dorsal foregut (D). (E-F') Double immunofluorescence of dorsal foregut region. The border between the epithelium and mesenchyme is indicated with a broken line. In the wild type control, Isl1 labels the mesenchyme and a few epithelial cells intermingled with the Pdx1⁺ dorsal pancreas anlage (E,E'). Upon *Rdh10* inactivation, the dorsal foregut epithelium is thinner, more Isl1⁺ epithelial cells can be seen, and surrounding Isl1⁺ mesenchymal cells are reduced (F,F').

dp, dorsal pancreas; li, liver; st, stomach; vp, ventral pancreas. Scale bars are 50 μ m.

Figure 3. *Rdh10* null-mutant embryos have a hypoplastic ventral pancreas

(A-F) Pancreatic buds of sectioned E11.5 embryos. Pdx1, Ptf1a, and Nkx6-1 (triple staining in A,C,E) and Sox9 (B,D,F) immunoreactivity labels the multipotent progenitor cells in the wild type control and mutant embryo.

(G) The proportion of Gcg⁺ cells is not significantly different between wild type control and mutant ventral pancreata at E10.5 and E12.5. ($n \geq 3$).

(H,I) Quantitation of size (H) and cell proliferation (I) of the developing ventral pancreas at E10.5, E11.5, and E12.5. Note that at each analyzed stage, the ventral pancreas of *Rdh10*^{-/-} embryos is around half the size compared to their wild type control siblings, and the proportion of pH3⁺ proliferating cells is not significantly altered. The number of experiments per sample was $n \geq 3$.

(J-K'') Expression of cell polarity markers in the ventral pancreas at E11.5. Mucin1 is an apical, E-cadherin a basolateral, and Laminin a basal epithelial marker. The arrowhead demarcates Mucin1⁺ microcolumn in the wild type control pancreas (J,J'). The sibling knockout lacks microcolumn structures (K,K'), while the E-cadherin⁺ pancreatic epithelium and Laminin⁺ basal lamina are not affected.

(L-M'') Reduced branching and decreased Mucin1⁺ tubular structures in the ventral pancreas of *Rdh10*-deficient compared to wild type control embryos at E12.5.

dp, dorsal pancreas; il, intestinal lumen; ml, microlumen; pH3, phosphorylated histone 3; vp, pancreas. The p-value is $** < 0.01$. Scale bars are 50 μm .

Figure 4. *Foxa2*-Cre recombinase-driven *Rdh10* knockout stimulates lethality, growth retardation and lowered blood glucose levels

(A) Frequency of genotypes from interbreedings between *Foxa2*^{Cre/+};*Rdh10*^{+/-} males and *Rdh10*^{F/F} females. The survival rate indicates the percentage of alive versus expected genotypes according to Mendelian laws. Note that the survival rate of *FRKO* mice is equal to that of *Rdh10*^{F/+} control and *FRhet* siblings at E18.5, but reduced to 38.5% at P7. For the sake of clarity the heterozygous *Rdh10*^{F/+} genotype is not shown. The number of survivors per sample is indicated on top of the columns.

(B) *FRKO* embryos have the same size as *FRhet* littermates at E15.5 ($n \geq 18$), but are significantly smaller at E18.5 ($n \geq 9$) and P7 ($n \geq 6$).

(C) Pups at P7. Note the smaller size of the *FRKO* (bottom) compared to its *FRhet* sibling (top).

(D) The blood glucose level in *FRKO* pups is decreased compared to *FRhet* littermates and *Foxa2*^{Cre/+};*Rdh10*^{+/+} control mice at P7 ($n \geq 15$).

p-values are $*** < 0.001$, $** < 0.01$, and $* < 0.05$.

Figure 5. Downregulation of *Rdh10* in the endoderm reduces the dorsal pancreas and its content of early Gcg⁺ and Ins⁺ cells in a retinoic acid-dependent manner

(A-D) Immunofluorescence analysis of Gcg and Ins expression in E12.5 dorsal pancreata of *FRKO* and *FRhet* control embryo. LacZ staining confirms specific *Foxa2*-Cre recombinase activity in the *Rosa26R-lacZ*^{F/+} pancreas epithelium (A', B'). Arrowheads label Gcg⁺Ins⁺ cells.

(E, F) Maternal supplementation of 0.4 mg retinal (E) and 0.2 mg retinoic acid per g food (F) from E8.5 until the stage of analysis at E12.5 in *FRKO* dorsal pancreata.

(G-I) Quantitation of dorsal pancreas size and hormone-expressing cells at E12.5. Note that *FRKO* dorsal pancreata are almost half as large as their *Rdh10*^{F/+} control and *FRhet* siblings, and that the proportion of Gcg⁺ and Ins⁺ cells is around 50% reduced. Supplemented retinal and retinoic acid

rescue the reduction of both size and hormone⁺ cells in *FRKO* dorsal pancreata in at least four experiments ($n \geq 4$).

(J,K) *FRKO* ventral pancreata keep their normal size and proportion of Gcg⁺ cells. Retinoid supplementation has no significant effect on mutant ventral pancreata ($n \geq 4$).

dp, dorsal pancreas. p-values are *** <0.001 , ** <0.01 , and * <0.05 . Scale bars are 50 μ m.

Figure 6. Endodermal *Rdh10* depletion reduces the expression of endocrine-specific transcription factors during the primary transition

(A,B) Ngn3 immunoreactivity labels the nuclei of pro-endocrine cells (arrowheads) in the dorsal pancreas of *FRhet* control and *FRKO* embryos at E11.5.

(C) *FRKO* reduces the proportion of Ngn3⁺ cells by 35% in the dorsal pancreas and has no significant effect in the ventral pancreas ($n \geq 3$).

(D-G) Immunofluorescence analysis in *FRhet* control and *FRKO* embryos at E12.5. Pax6⁺ and MafB⁺ cell nuclei cluster in Gcg⁺ cells (arrowheads) but also appear in Gcg⁻ cells of the Pdx1⁺ dorsal pancreatic epithelium (arrows).

(H,I) In the dorsal pancreas of *FRKO* embryos, the relative numbers of both Pax6⁺Gcg⁺ and Pax6⁺Gcg⁻ cells are reduced by ~50% compared to *Rdh10*^{F/+} and *FRhet* control siblings. Pax6 expression in the ventral pancreas is not significantly affected. The number of experiments per sample was $n \geq 3$.

dp, pancreas. p-values are ** <0.01 and * <0.05 . Scale bars are 50 μ m.

Figure 7. *Rdh10* is important for definitive endocrine cell differentiation in the dorsal pancreas

(A-D) Quantitative PCR analysis in extracted pancreata at E15.5 and E18.5. mRNA levels of *Rdh10*, *Gcg*, *Ins*, and *Ppy* are reduced, while *Amy*, *Cpa1*, and *Ghrl* are not changed in *FRKO* embryos compared to *FRhet* control littermates. *Sst* expression is unaffected at E15.5, but reduced at E18.5.

The number of embryos per genotype was $n \geq 4$.

(E-H) At E15.5, the *FRKO* dorsal pancreas is smaller and contains less Gcg- and Ins-immunopositive cells than the *FRhet* control sibling, while the relative number of Sst⁺-cells is not affected. The size of the mutant ventral pancreas and its content of hormone-producing cells are not significantly changed ($n \geq 3$).

p-values are *** <0.001 and * <0.05 . Scale bars are 50 μm .

Figure 8. Rdh10 functions in the commitment of definitive endocrine cells

(A) qPCR analysis of extracted pancreata at E15.5 and E18.5. Note increase of *Rbp4* mRNA level in the *FRKO* compared to the *FRhet* control. The number of experiments per genotype was $n \geq 6$.

(B-C'') Immunofluorescence analysis of E14.5 dorsal pancreata in *FRhet* control and *FRKO* embryos. Note Ngn3^{LO} (arrow) and Ngn3^{HI} cell nuclei (arrowhead). The open arrowhead indicates a nucleus with overlapping Ngn3 and Pax6 expression.

(D) The number of Ngn3^{HI} cells is reduced in the *FRKO* dorsal pancreas, and the number of Ngn3^{LO} cells increased in the *FRKO* ventral pancreas in at least three experiments ($n \geq 3$).

(E) The proportion of Pax6⁺ cells is not significantly changed in both dorsal and ventral *FRKO* pancreata ($n \geq 3$).

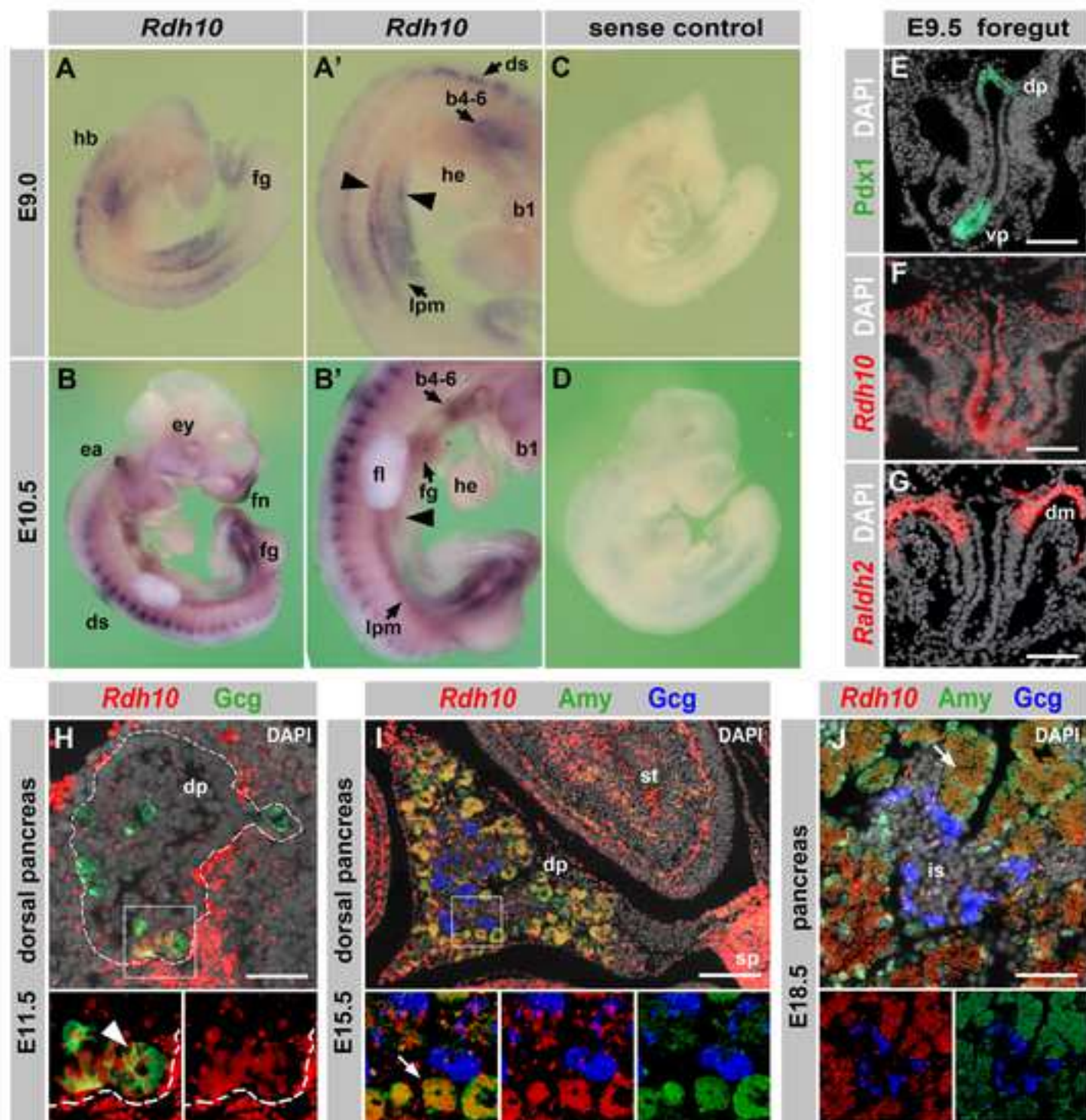
(F,G) qPCR analysis. Note reduction of *Arx*, *Nkx6-1*, and *MafA*, while *Pax4*, *Pax6*, and *GLUT2* mRNA levels are increased in the E18.5 *FRKO* compared to *FRhet* control pancreas ($n \geq 6$). dp, dorsal pancreas.

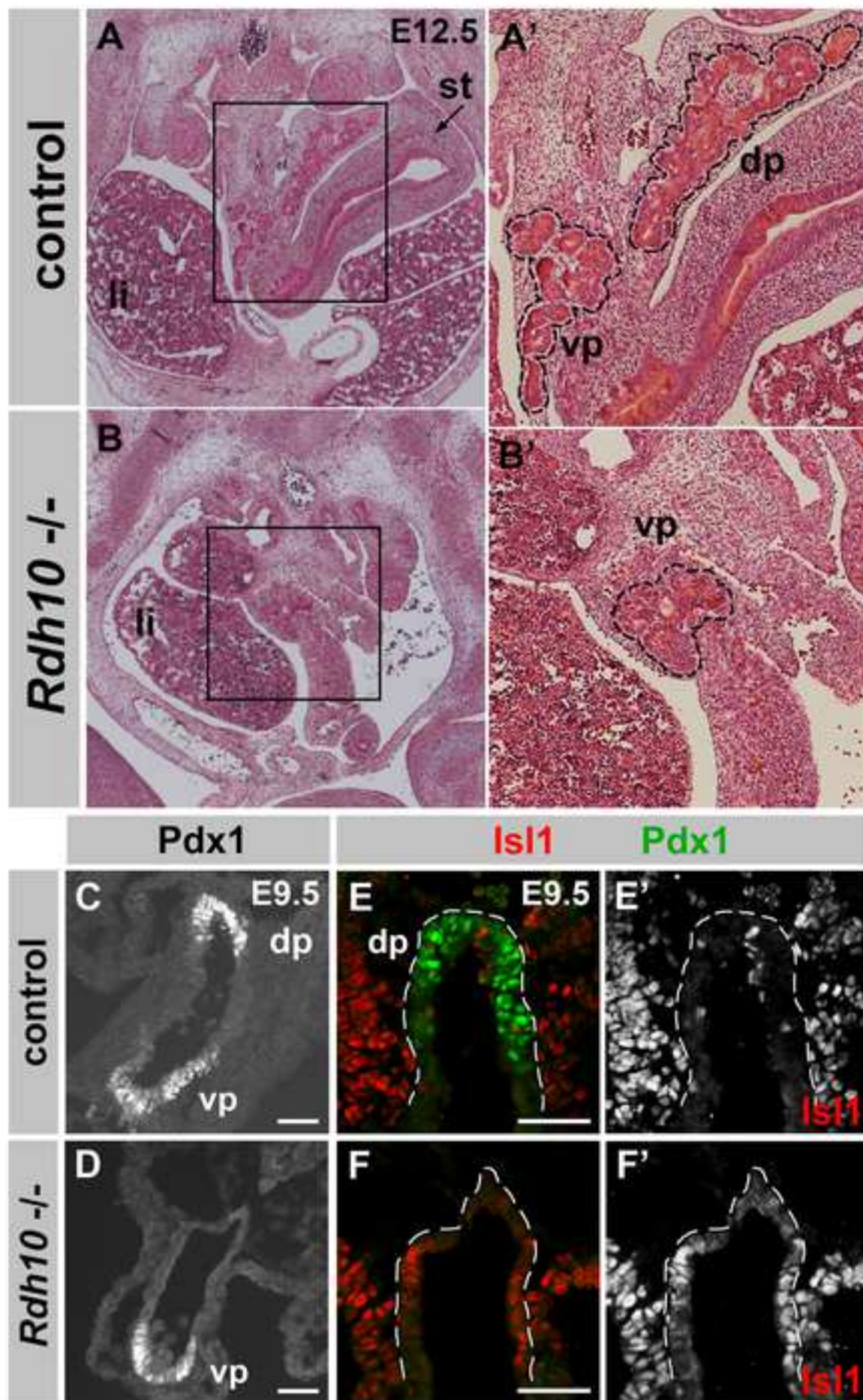
p-values are ** <0.01 and * <0.05 . Scale bars are 50 μm .

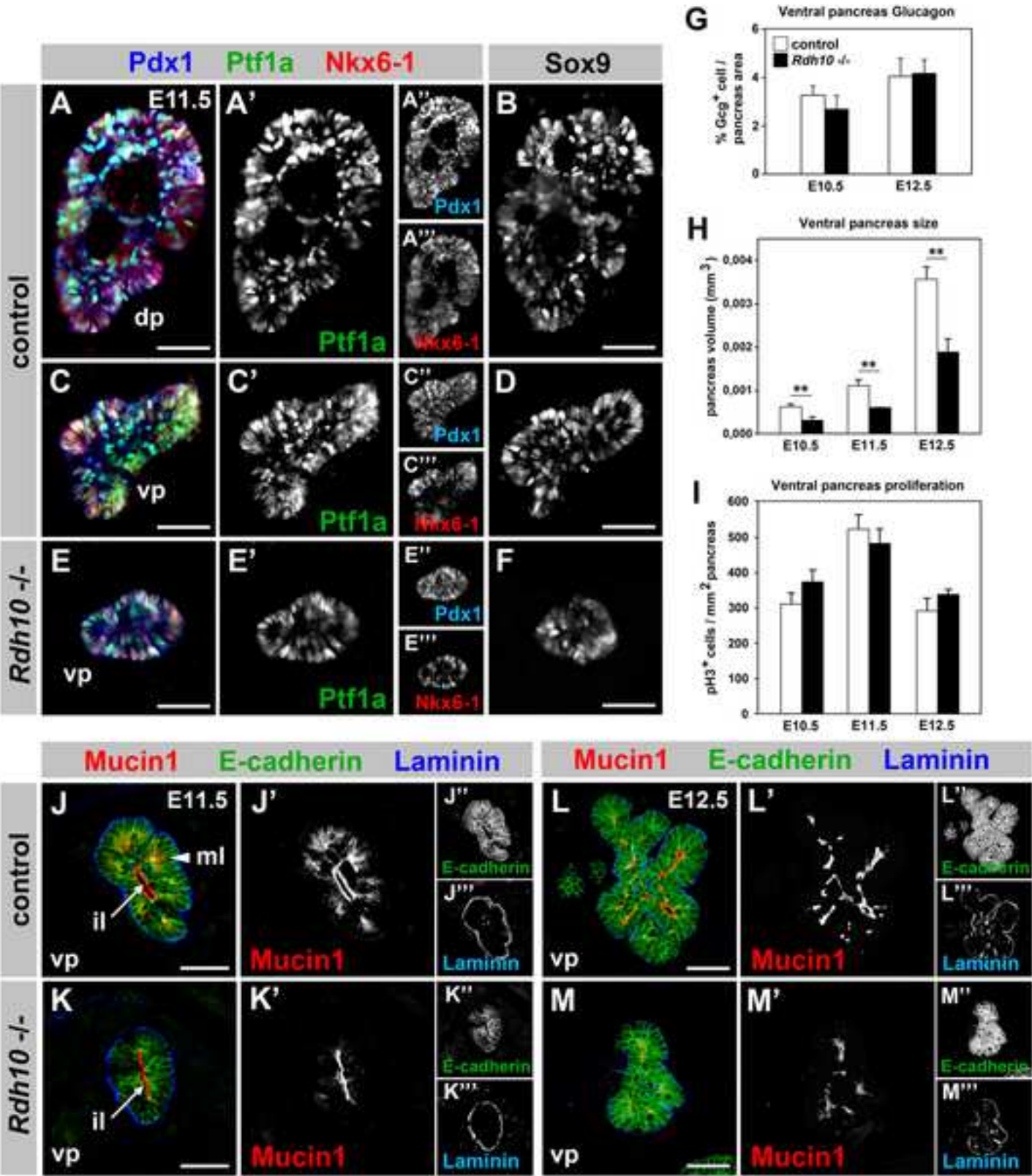
Figure 9. Model for the interaction of Rdh10 and retinal dehydrogenases during RA biosynthesis in pancreatic endocrine cell differentiation.

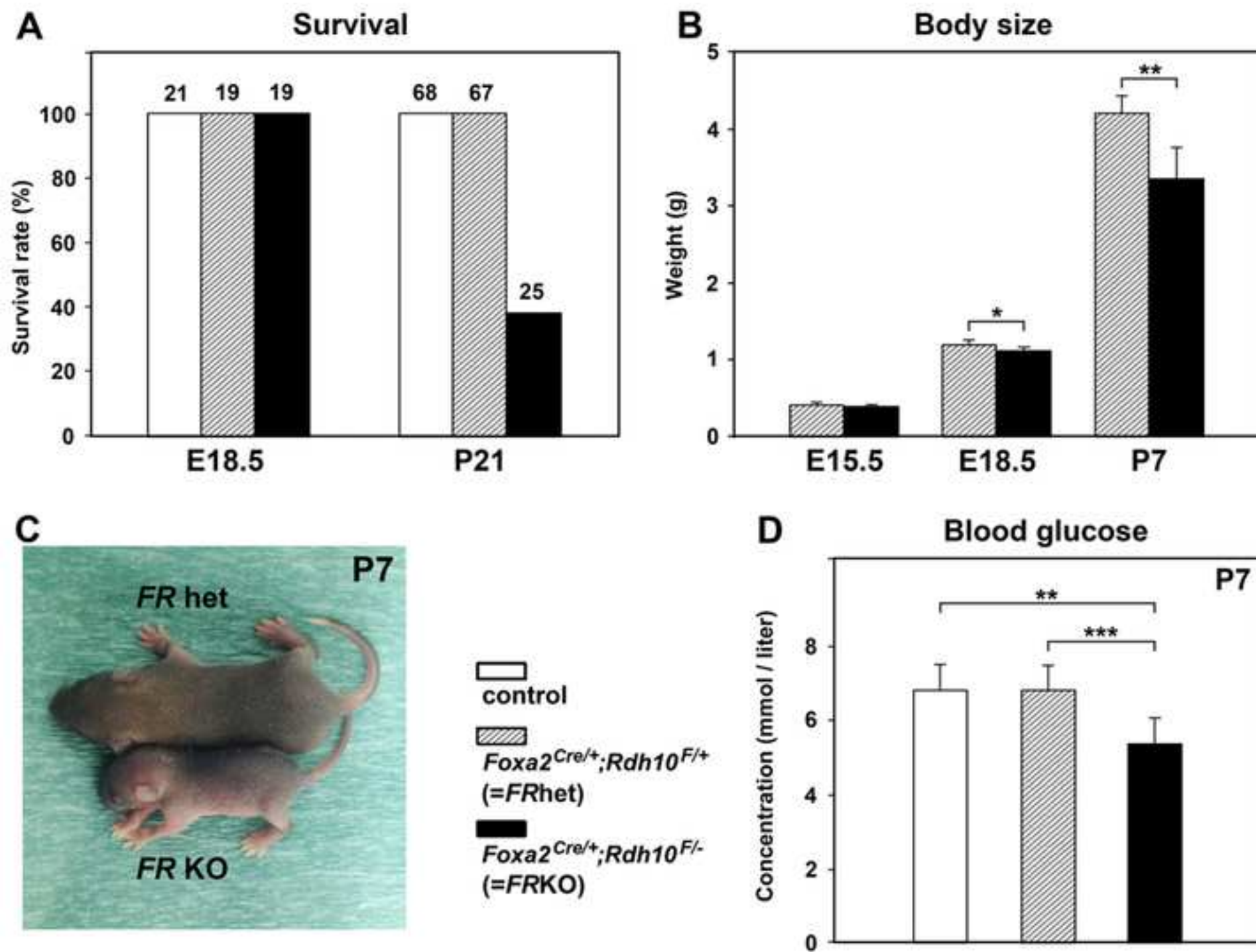
(A) Primary transition in the dorsal foregut at E9.5. Vitamin A released from the dorsal aorta is metabolized by adjacent epithelial and mesenchymal Rdh10 to retinal, which in turn is further converted by mesenchymal Raldh2 to bioactive RA. A gradient of RA induces early endocrine cell fate in dorsal pancreas epithelium.

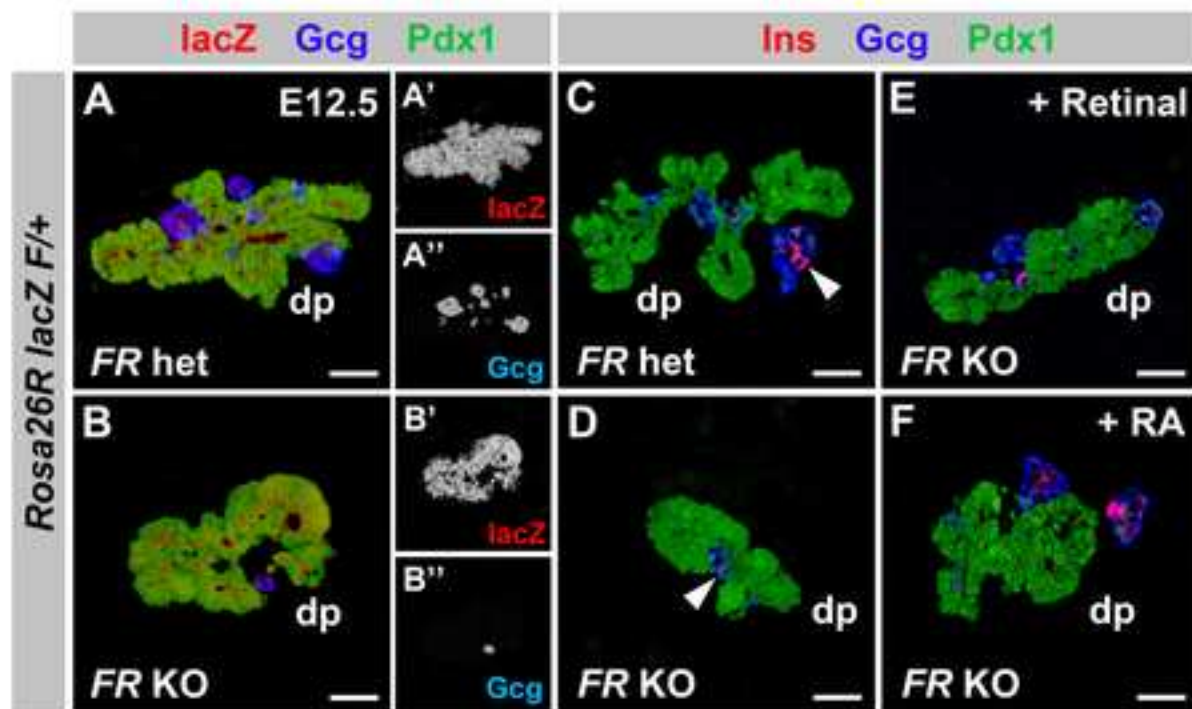
956 (B) Secondary transition in the dorsal pancreas at E15.5. Vitamin A from pancreatic blood vessels is
957 bound by Rbp4 close to endocrine cell clusters and delivered to adjacent acinar cells, in which Rdh10
958 and Raldh1 produce RA. RA in turn promotes initiation and terminal differentiation of α - and β -cells.



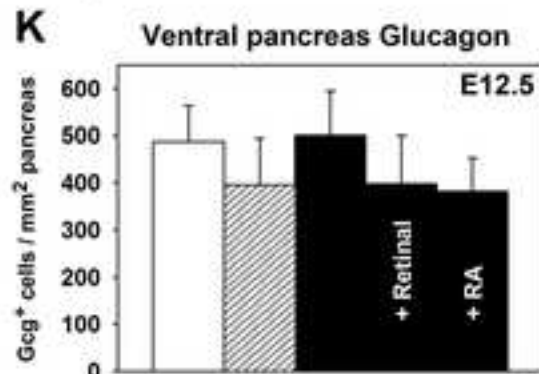
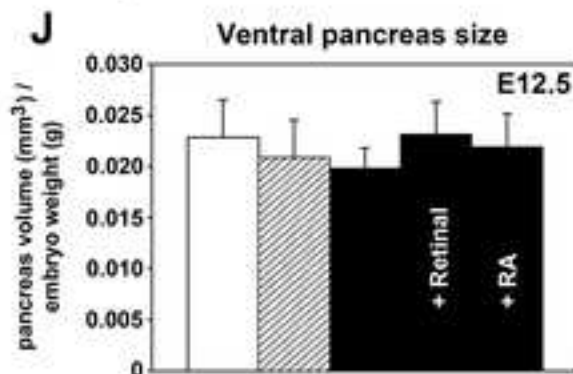
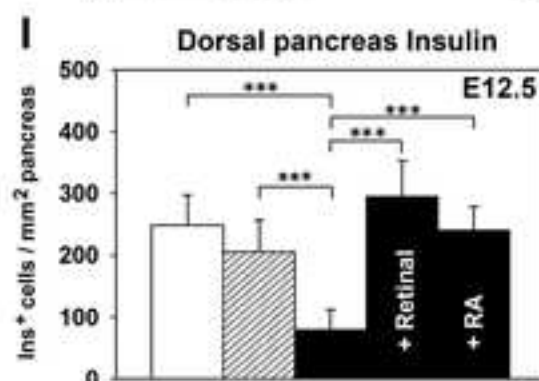
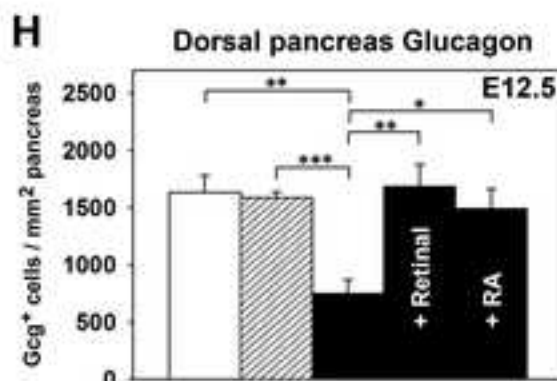
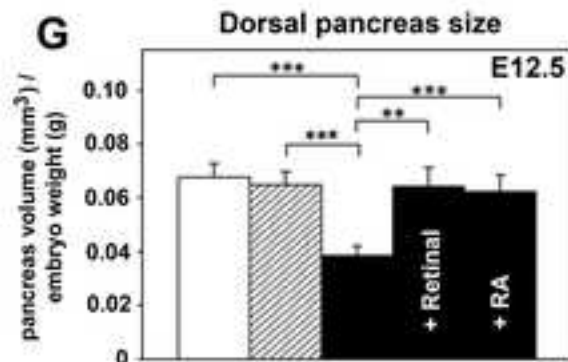


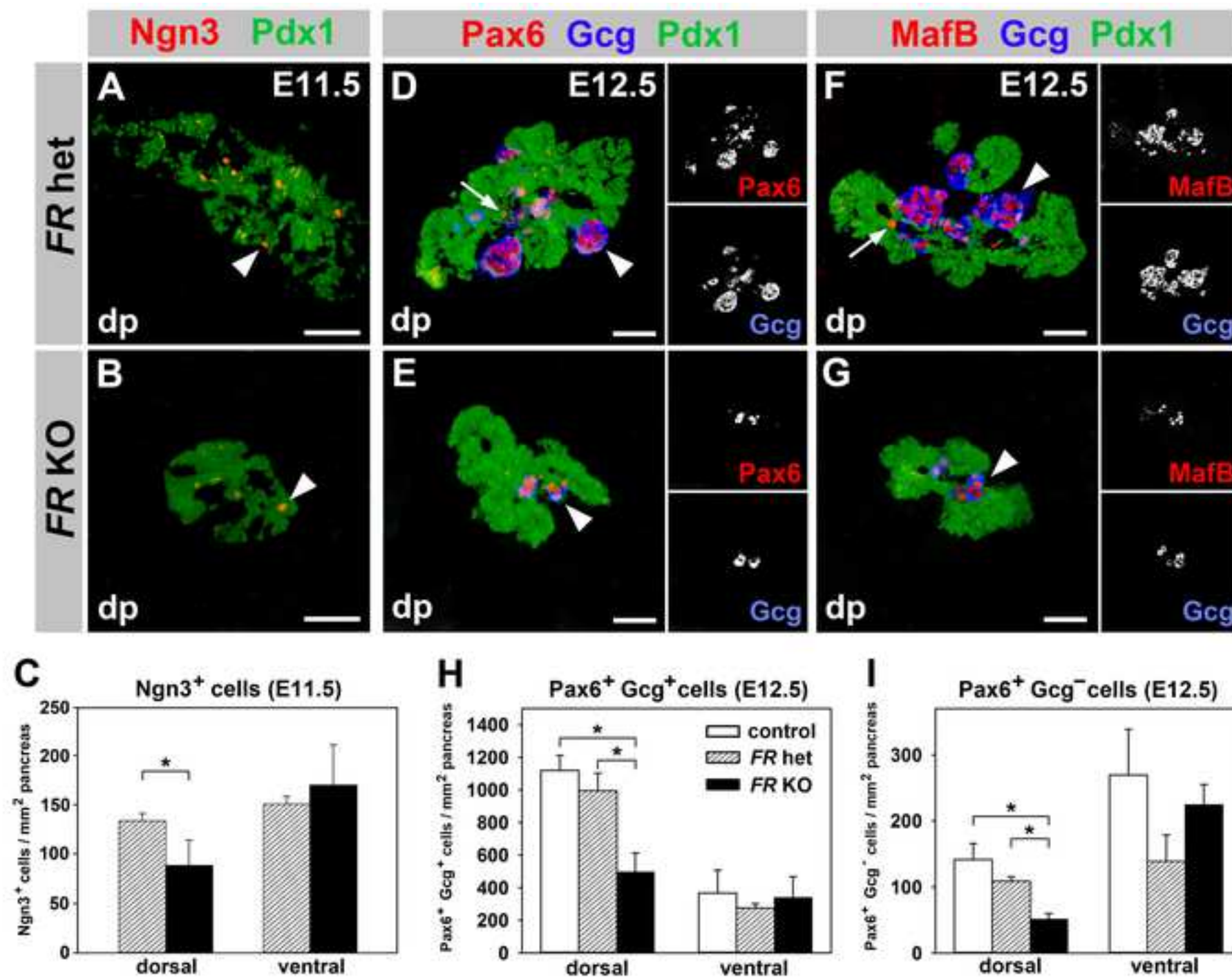


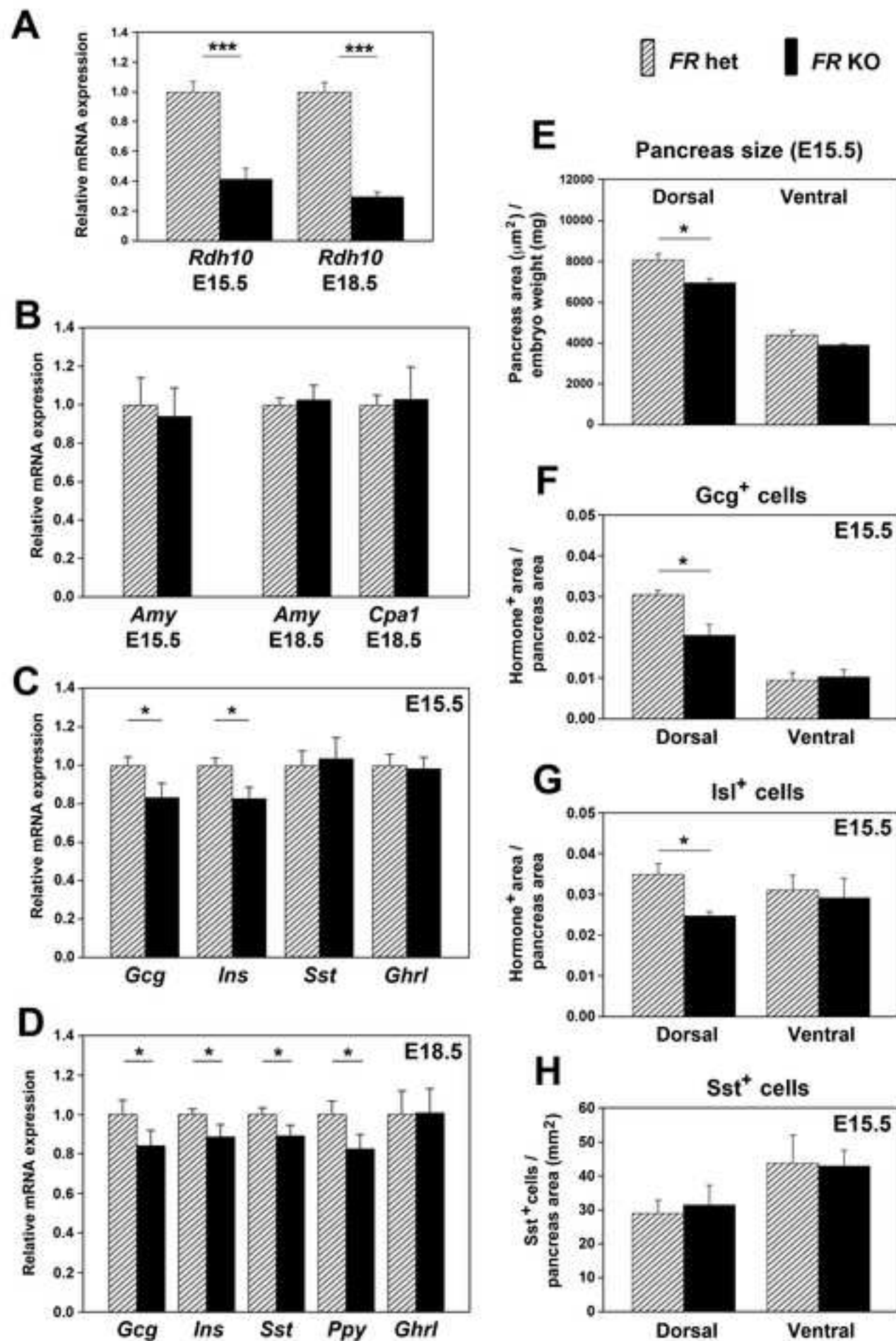


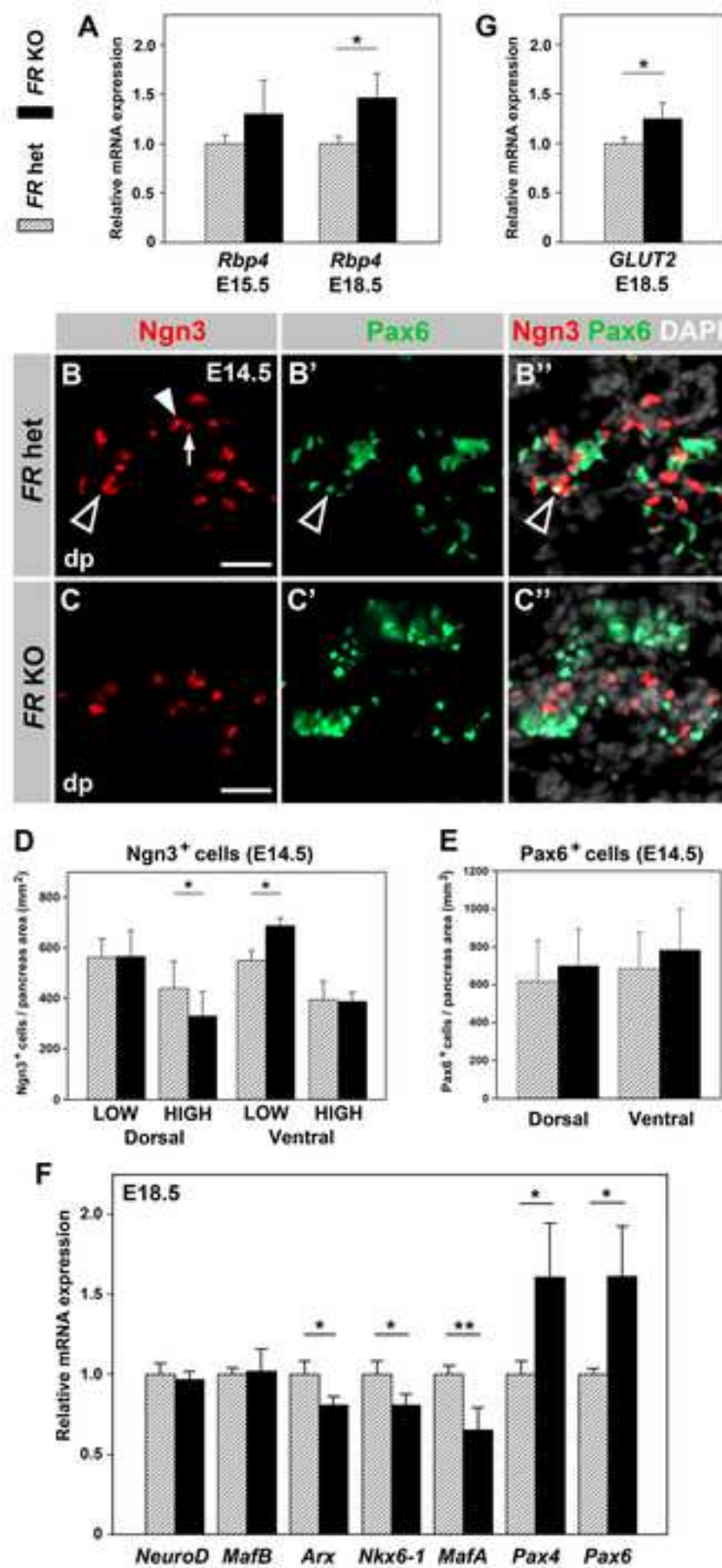


control
Foxa2^{Cre/+};Rdh10^{F/+} (=FR het)
Foxa2^{Cre/+};Rdh10^{F/-} (=FR KO)

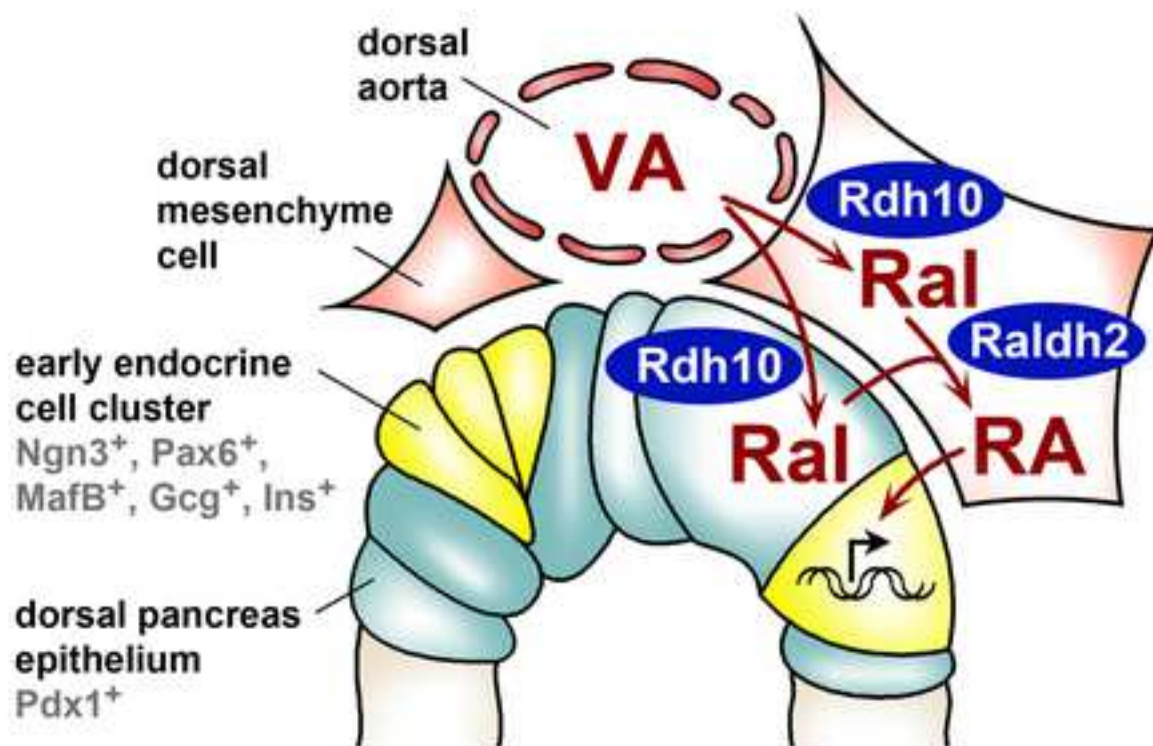








A Dorsal foregut (E9.5)



B Dorsal pancreas (E15.5)

